FINITE ELEMENT METHOD BASED SIMULATION, DESIGN, AND RESONANT MODE ANALYSIS OF RADIO FREQUENCY BIRDCAGE COILS USED IN MAGNETIC RESONANCE IMAGING

A THESIS

SUBMITTED TO THE DEPARTMENT OF ELECTRICAL AND

ELECTRONICS ENGINEERING

AND THE GRADUATE SCHOOL OF ENGINEERING AND SCIENCE

OF BILKENT UNIVERSITY

IN PARTIAL FULFILLMENT OF THE REQUIREMENTS

FOR THE DEGREE OF

MASTER OF SCIENCE

By

Necip Gürler

August, 2012

I certify that I have read this thesis and that in my opinion it is fully adequate, in scope and in quality, as a thesis for the degree of Master of Science.

Prof. Dr. Yusuf Ziya İder(Advisor)

I certify that I have read this thesis and that in my opinion it is fully adequate, in scope and in quality, as a thesis for the degree of Master of Science.

Prof. Dr. Ergin Atalar

I certify that I have read this thesis and that in my opinion it is fully adequate, in scope and in quality, as a thesis for the degree of Master of Science.

Prof. Dr. Nevzat Güneri Gençer

Approved for the Graduate School of Engineering and Science:

Prof. Dr. Levent Onural
Director of the Graduate School

ABSTRACT

FINITE ELEMENT METHOD BASED SIMULATION, DESIGN, AND RESONANT MODE ANALYSIS OF RADIO FREQUENCY BIRDCAGE COILS USED IN MAGNETIC RESONANCE IMAGING

Necip Gürler
M.S. in Electrical and Electronics Engineering
Supervisor: Prof. Dr. Yusuf Ziya İder
August, 2012

Radio Frequency (RF) birdcage coils are widely used in Magnetic Resonance Imaging (MRI) since they can generate very homogeneous RF magnetic field inside the coil and have high signal-to-noise ratio (SNR). In practice, designing a birdcage coil is a time-consuming and difficult task. Calculating the capacitance value, which is necessary for the coil to resonate at the desired frequency, is the starting point of the design process. Additionally, it is also important to know the complete resonance frequency spectrum (or resonant modes) of the birdcage coil that helps the coil designers to be sure that working mode is far away from the other modes and so that tuning and matching procedures of the coil can be done without interfering with the other modes. For this purpose, several studies have been presented in the literature to calculate the capacitance value and the resonant modes of the birdcage coil. Among these studies, *lumped circuit element model* is the most used technique in capacitance and resonant modes calculations. However, this method heavily depends on the inductance calculations which are made under quasi-static assumptions. As a consequence of this assumption, error in the calculations increases as the frequency increases to a point at which the wavelengths are comparable with the coil dimensions. Additionally, modeling the birdcage coil in a 3D simulation environment and making electromagnetic analysis in the volume of interest is also important in terms of observing the electromagnetic field distributions inside the coil. In this thesis, we have proposed three different Finite Element Method (FEM) based simulation methods which are performed using the developed low-pass and high-pass birdcage coil models in COMSOL Multiphysics. One of these methods is the FEM based optimization method in which magnitude of the port impedance or variance of H^+ is used as the objective function and the capacitance value is used as the control

variable. This is a new method proposed for calculating the capacitance value of the birdcage coils. The other method is the eigenfrequency analysis which is used to determine not only the resonant modes of the birdcage coil but also the electromagnetic fields distributions inside the coil at these resonant modes. To the best of our knowledge, FEM based eigenfrequency analysis of a birdcage coil is also a new study in the field of MRI. The last method is the frequency domain analysis which is used solve for the electromagnetic fields of a birdcage coil for the specified frequency (or frequencies). One can also use this method to estimate Specific Absorption Rate (SAR) at any object inside the coil. To make these three simulation methods easily and according to the user-specified parameters, we have developed two software tools using MATLAB which have also graphical user interface (GUI). In order to compare the results of the proposed methods and the results of the methods that use lumped circuit element model with the experimental results, we have constructed two handmade birdcage coils and made measurements for different capacitance values. Then, we have compared the measured resonant modes with the calculated resonant modes; used capacitance values with the calculated capacitance values. For the worst case (in which the frequency is the highest), proposed FEM based eigenfrequency analysis method calculates the resonant modes with a maximum of 10% error; proposed FEM based optimization method calculates the necessary capacitance values with 20-25% error. Methods which use lumped circuit element model, on the other hand, calculate the resonant modes and capacitance values with 50-55% error for the worst case.

Keywords: RF Birdcage Coils, Finite Element Method, Lumped Circuit Element Model, Capacitance Calculation, Frequency Domain Analysis, Eigenfrequency Analysis.

ÖZET

MANYETİK REZONANS GÖRÜNTÜLEMEDE KULLANILAN RADYO FREKANSI KUŞKAFESİ SARGILARIN SONLU ELEMANLAR YÖNTEMİNE DAYALI BENZETİMİ, DİZAYNI, VE REZONANS MOD ANALİZİ

Necip Gürler
Elektrik ve Elektronik Mühendisliği Bölümü, Yüksek Lisans
Tez Yöneticisi: Prof. Dr. Yusuf Ziya İder
Ağustos, 2012

Radyo Frekansı (RF) kuşkafesi sargıları, sargı içerisinde oluşturdukları homojen RF manyetik alan ve sahip oldukları yüksek işaret gürültü oranı (İGO) sebebiyle Manyetik Rezonans Görüntülemede (MRG) oldukça sık kullanılır. Pratikte, kuşkafesi sargılarının tasarımı zor ve zaman alan bir iştir. Sargının istenilen frekansta rezonansa girmesi için gerekli kapasitans değerinin hesaplanması, tasarım işleminin ilk aşamasıdır. Ayrıca, kuşkafesi sargıların tüm rezonans modlarının bilinmesi de önemlidir. Bu sayede, sargı tasarımcıları sargının çalışma frekansının diğer rezonans modlarından uzakta olduğundan emin olur ve sargının frekansının ayarlanması ve empedans eşlenmesi diğer rezonans modlarına karışmadan yapılabilir. Bu amaçla, kapasitans değerini ve rezonans modlarını hesaplamak için litaratürde bir çok çalışma yapılmıştır. Bu çalışmalar arasında, *toplu öğeli devre modeli* kapasitans ve rezonans modu hesaplamaları için en çok kullanılan tekniktir. Ancak bu yöntem, yarı-statik varsayımıyla yapılan endüktans hesaplarına aşırı derecede bağlıdır. Bu varsayımın bir sonucu olarak, dalgaboyunun sargı boyutlarına yaklaştığı frekanslara doğru gidildikçe hesaplamalardaki hatalar artmaktadır. Ayrıca, kuşkafesi sargıların üç boyutlu bir simülasyon ortamında modellenmesi ve istenilen bölgede elektromanyetik analizlerin yapılması, sargı içerisindeki elektromanyetik alan dağılımlarının gözlemlenebilmesi açısından önemlidir. Bu tezde, COMSOL Multiphysics'de oluşturulan alçak-geçirgen ve yüksek-geçirgen kuşkafesi sargı modelleri kullanılarak yapılan Sonlu Elemanlar Yöntemine (SEY) dayalı üç farklı simülasyon yöntemi önermekteyiz. Bu yöntemlerden biri, içerisinde port empedansının genliğinin veya H^+ varyansının amaç fonksiyonu olarak; kapasitans değerinin

ise kontrol değişkeni olarak kullanıldığı SEY bazlı optimizasyon yöntemidir. Bu yöntem, kuşkafesi sargıların kapasitans değerinin hesaplanması için önerilen yeni bir yöntemdir. Diğer yöntem, kuşkafesi sargıların sadece rezonans modlarının belirlenmesinde değil bu rezonans modlarındaki sargı içerisinde oluşan elektromanyetik alan dağılımlarının bulunmasında da kullanılan özfrekans analizidir. Bilgimiz dahilinde, kuşkafesi sargıların SEY bazlı özfrekans analizi de MRG alanındaki yeni bir çalışmadır. Son yöntem ise, bir kuşkafesi sargısının elektromanyetik alanlarının belirtilen bir (ve ya daha çok) frekansta çözümü için kullanılan frekans bölgesi analizidir. Bu yöntem, sargı içerisindeki herhangi bir cismin özgül soğurma hızı (ÖSH) dağılımının bulunması için de kullanılabilir. Bu üç simülasyon yönteminin kolayca ve kullanıcı tarafından girilen parametrelere göre uygulanabilmesi için, MATLAB kullanılarak grafiksel kullanıcı arayüzü de olan iki yazılım aracı geliştirdik. Önerilen yöntemlerin sonuçları ve toplu öğeli devre modeli kullanan yöntemlerin sonuçlarını, deneysel sonuçlar ile karşılaştırmak için iki adet kuşkafesi sargısı yaptık ve farklı kapasitans değerleri için ölçümler aldık. Daha sonra ölçülen rezonans modları ile hesaplanan rezonans modlarını; kullanılan kapasitans değerleri ile hesaplanan kapasitans değerlerini karşılaştırdık. En kötü durum için (frekansın en yüksek olduğu durum), önerilen SEY bazlı özfrekans analizi yöntemi rezonans frekanslarını en çok %10 hata ile; önerilen SEY bazlı optimizasyon yöntemi ise kapasitans değerlerini %20-25 hata ile hesaplamaktadır. Toplu öğeli devre modelini kullanan yöntemler ise rezonans modları ve kapasitans değerlerini, en kötü durum için %50-55 hata ile hesaplamaktadır.

Anahtar sözcükler: RF Kuşkafesi Sargıları, Sonlu Elemanlar Yöntemi, Toplu Öğeli Devre Modeli, Kapasitans Hesaplama, Frekans Bölgesi Analizi, Özfrekans Analizi.

Acknowledgement

First and foremost, I would like to express my deep and sincere gratitude to my supervisor Prof. Dr. Yusuf Ziya İder for his invaluable guidance and encouragement throughout my M.Sc. study. His wide knowledge and his logical way of thinking have been of great value for me. Beyond his role as an academic advisor, he has been a very good friend. Undoubtedly, I am fortunate to work with an advisor like him.

I would like to thank Prof. Dr. Ergin Atalar and to Prof. Dr. Nevzat Güneri Gençer for kindly accepting to be a member of my jury.

I wish to thank Taner Demir for his help during the experiments in National Magnetic Resonance Research Center (UMRAM).

I would like to express my thanks to the The Scientific and Technological Research Council of Turkey (TÜBİTAK) for providing financial support during my M.Sc. study.

Very special thanks goes to my office mates Ömer Faruk Oran, Fatih Süleyman Hafalır, Mustafa Rıdvan Cantaş, and Merve Begüm Terzi for the sleepless nights we were working together before deadlines, and for all the fun we have had in the last two years. I would like to extend my thanks to my room mate Salim Arslan for his friendship.

Last not least, I wish to express my deep gratitude to my parents who have grown me up and supported me through all my life. Also I would like to thank my sister, Gizem, for her lovely support. Of course, I am indebted to my girlfriend Ayça Atasoy for her unconditional love, invaluable support, motivation and understanding.

Contents

List of Figures

List of Tables

Chapter 1

INTRODUCTION

Radio Frequency (RF) coils are one of the key components in Magnetic Resonance Imaging (MRI). They are responsible for two primary functions in MRI. One of them is to generate rotating RF magnetic field (B_1) in the transverse plane in the volume of interest. This rotating B_1 field which is perpendicular to main magnetic field (B_0) excites the nuclei (spins) in the object at the Larmor frequency. The other function of RF coils is to receive signals induced by precessing of nuclear spins. These two functions are called excitation (transmission) and reception respectively.

RF coils can be divided into three groups according to the functions they serve: transmit only, receive only and transmit/receive coils. For the transmit RF coils, it is desired that they are able to generate homogeneous B_1 field in the volume of interest at the desired operating frequency. Providing good homogeneity along with less power consumption is highly preferable for the transmit coils. Saddle coils, transverse electromagnetic (TEM) coils and birdcage coils can be used as transmit coils. For the receive coils, on the other hand, it is desired that they are able to receive signals with a high signal-to-noise ratio (SNR). Additionally, receive sensitivity of the coil is required to be close to uniform. Phase array coils and surface coils can be given as examples of receive coils. Some coil types are shown in Figure 1.1.

Figure 1.1: a) Surface coils b) Phased array coil c) Birdcage coil

In addition to above requirements given for RF transmit and receive coils separately, there are other important requirements for the RF coils such as having good filling factor, minimum coil losses, quadrature excitation and reception capability. In this thesis, birdcage coils, which is one of the most used RF coil type in MRI and having the most of the requirements given above, are discussed in details. In the following two introductory sections, brief information on RF birdcage coils and review of previous studies about designing and simulating a birdcage coil are given. After these sections, objective and scope of the thesis are stated. Finally, organization of the thesis is described.

1.1 RF Birdcage Coils

RF birdcage coils have been widely used in MRI because they can generate a very homogeneous RF magnetic field in the volume of interest with a high SNR [1]. They can also be used for quadrature excitation and reception because of its cylindrical symmetry. When a birdcage coil is driven as quadrature, -driving a birdcage coil from two ports that are geometrically 90° apart from each other and one of the ports having signal with a 90° phase shift- it generates circularly polarized field inside the coil at the desired frequency. Additionally, necessary RF transmission power required in quadrature excitation is half of the RF transmission power required in linear excitation. Furthermore, SNR increases by a factor of $\sqrt{2}$ in quadrature excitation relative to the linear excitation case [2].

Birdcage coils or resonators consist of two circular conductive loops referred to as end rings, N conductive straight elements referred to as rungs (or legs) and lumped capacitors on the rungs or end rings or both. According to the location of these capacitors on the coil geometry, there are three types of birdcage coils: low-pass, high-pass and band-pass birdcage coils. They are illustrated in Figure 1.2. Note that, band-pass birdcage coils are not discussed in this thesis.

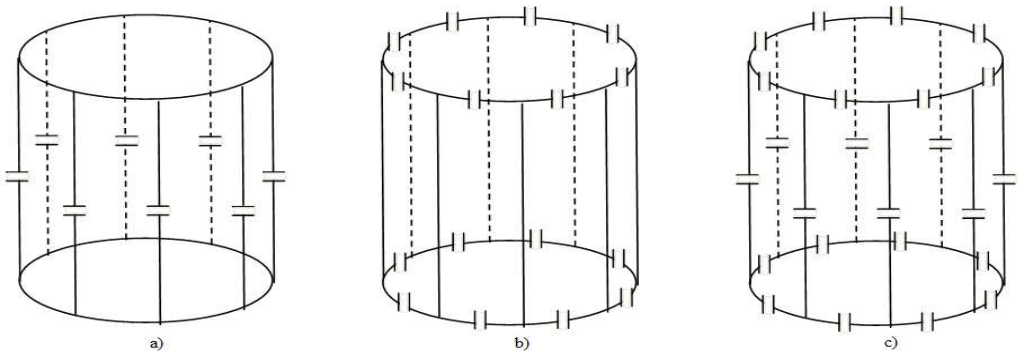

Figure 1.2: Illustration of birdcage coils. a) Low-pass b) High-pass c) Band-pass

A birdcage coil with N number of legs and equal valued capacitors has $N/2$ distinct resonant modes in which the mode number $m = 1$, lowest frequency resonant mode for low-pass birdcage coils or highest frequency resonant mode for high-pass birdcage coils, generates a sinusoidal current distribution in the rungs resulting in a homogeneous B_1 field inside the coil. Resonant modes, $m = 1, 2, ..., (\frac{N}{2})$, are called degenerate modes or degenerate mode pairs that are actually two modes having the same resonant frequency but represented with the same m and produce B_1 field which is perpendicular to each other. Quadrature excitation and reception mentioned in the first paragraph of this section is provided by these two orthogonal resonant modes. Since they produce B_1 fields that are perpendicular to each other, a birdcage coil can be driven from two ports that are geometrically 90° apart from each other and with signals whose phases differs by 90° in order to obtain a constant rotating B_1 field at the desired frequency. There is also another resonant mode for the birdcage coils called co-rotating/anti-rotating (CR/AR) mode [3]. This mode, $m = 0$, is a bit different than the other modes because the currents flow only in the end rings so that there is no transverse

magnetic field in the volume of interest. If the currents in each end ring are in the same direction, this is called co-rotating (CR) mode and if the currents are in opposite direction, this is called anti-rotating (AR) mode. In low-pass birdcage coils, CR/AR mode degenerates at zero frequency (DC), whereas in high-pass birdcage coils $m = 0$ degenerates at highest frequency in the resonance frequency spectrum.

As mentioned above, in order to generate a desired homogeneous B_1 field in the N-leg birdcage coil at Larmor frequency, currents in the rungs must be proportional to $sin\theta$ (or $cos\theta$), that corresponds to $m = 1$ mode, where θ values can be expressed as

$$\theta = \frac{360}{N} i \qquad\qquad i = 1, 2..., N \tag{1.1}$$

Producing sinusoidal current distribution in the rungs as well as the desired homogeneous B_1 field at the operating frequency is achieved by using the correct capacitance value for the capacitors placed on the rungs or end rings. Therefore, finding the necessary capacitance value for the birdcage coil to resonate at the desired frequency is the starting point of designing a birdcage coil. Additionally, it is also important to know the complete resonance frequency spectrum of a birdcage coil that helps the coil designers to be sure that working mode is far away from the other modes and so that tuning the coil can be done without interfering with the other modes [4]. Furthermore, before the actual construction of the coil, geometrically modeling the coil in a 3D simulation environment and making electromagnetic analysis in the region of interest have importance in terms of observing the resonance behavior and other performance features of the coil such as B_1 field distribution inside the coil and specific absorption rate (SAR) in an arbitrary object. These electromagnetic analyses can also be used to produce simulated B_1 data inside the coil that can be compared with the experimental data later or that can be used as simulation data for electromagnetic tissue property mapping techniques such as Magnetic Resonance Electric Properties Tomography (MREPT).

1.2 Review of Previous Studies about Designing and Simulating a Birdcage Coil

Although construction of birdcage coils are based on the iterative procedures (tuning and matching), there are several techniques proposed in designing and simulating a birdcage coil in the literature. Note that, we mean calculating the necessary capacitance value or resonant modes of a birdcage coil by saying "designing a birdcage coil" and we mean solving for the electromagnetic fields of a birdcage coil by saying "simulating a birdcage coil".

One of the mostly used techniques for designing a birdcage coil is to use lumped circuit element model. In this model, rungs and end rings are first modeled as an inductor. Then, self inductances and mutual inductances of the rungs and end rings are calculated by using handbook formulas. Finally, the equivalent circuit model (LC network) is solved by using Kirchoff's voltage and current laws. Chin et al. presented a useful method to calculate the necessary capacitance value for given resonance frequency [5]. Tropp analyzed the low-pass birdcage resonator by using lumped circuit element model and perturbation theory [6]. Leifer, on the other hand, presented a method to calculate all resonant modes in the frequency spectrum by using discrete Fourier transform [3]. Pascone, performed analysis of both low-pass and high-pass birdcage coils by using lumped element transmission line theory [7]. Among these studies, the method presented in [5] is a bit different. In [5], necessary capacitance value is calculated for the given desired resonance frequency, whereas in other studies, capacitance value is known and resonance frequency (frequencies) is (are) calculated for the known capacitance value. Since the coil geometry and the desired resonance frequency are usually known parameters, method presented in [5] is very useful to calculate the starting capacitance value for the coil designers. However, there are some limitations in this method. First, coupling between opposite end rings is not considered. Therefore, accuracy of the calculated capacitance will decrease when the coil length gets shorter. Second, end ring segments are considered as straight lines when calculating the mutual inductance between these segments but in practice

this is not true. For this reason, error in calculating capacitance value will increase, when the number of legs in the coil decreases. Finally, self inductance, mutual inductance and capacitance calculations are made under the quasi-static assumptions. As a consequent of this assumption, error will increase when the desired resonance frequency increases to a point at which the wavelengths are comparable with the coil dimensions. This assumption is also used in other studies that use lumped circuit element model in order to analyze the birdcage coil. There is an important criterion, which is used for determining whether a wire can be modeled as lumped circuit element or not, which is given as [8]

$$length\ of\ wire \leq \frac{\lambda}{20} \tag{1.2}$$

where λ is the signal wavelength. According to the criterion given in Equation 1.2, if the coil length (or diameter) is larger than the one twentieth of the wavelength at the operating frequency, using lumped circuit element model in birdcage coil design will give unreliable results.

In addition to studies about designing a birdcage coil, there have been also studies on simulating a birdcage coil in the literature. A method introduced by Jin [9], first calculates the resonance modes of the coil by using lumped circuit element model. Than, it computes the currents in the rungs and end rings for each mode by solving generalized eigenvalue problem. Finally, it calculates the B_1 field for each mode inside the coil by using Biot-Savart's law. Since the method calculates both resonance frequencies for the given capacitor value and B_1 field distribution inside the coil, it can be used for both designing and simulating a birdcage coil. However, it makes heavy approximations while calculating the mutual inductances of the coil. As a result, accuracy of the calculated resonance frequencies as well as the B_1 field distribution inside the coil will be low.

On the other hand, there are 3D numerical methods such as finite element method (FEM), the finite difference time domain method (FDTD), and the method of moments (MoM) that can used to simulate birdcage coils in the literature [10, 11, 12, 13]. As mentioned in the first paragraph of this section, these methods have been used for solving the electromagnetic fields of a loaded or unloaded birdcage coils at the desired frequency. There are also software packages

based on these numerical methods such as COMSOL Multiphysics (COMSOL AB, Stockholm, Sweden), XFdtd (Remcom, PA, USA), HFSS (ANSYS, PA, USA) and SEMCAD X (SPEAG, Zurich, Switzerland). Using these software packages, loaded or unloaded birdcage coils can be modelled and electromagnetic field calculations inside the coil can be made accurately. As a result of these electromagnetic field simulations, researchers and coil designers have opportunity to investigate birdcage coils elaborately.

1.3 Objective and Scope of the Thesis

This thesis covers detailed analyses of FEM based design, simulation and resonant mode analysis of a birdcage coil using the developed FEM models of low-pass and high-pass birdcage coils in COMSOL Multiphysics.

As previously mentioned, when the wavelength is comparable with the order of coil dimensions at the operating frequency, capacitance values and resonant modes of the birdcage coil calculated by using lumped circuit element model are no longer trustworthy. In other words, when Equation 1.2 does not hold, calculations based on the lumped circuit element model will not be accurate and therefore, tuning and matching procedure of the coil will be time consuming and difficult. In order to calculate the initial capacitance value for the birdcage coils accurately even at higher frequencies, we have first built FEM models of low-pass and high-pass birdcage coils in COMSOL Multiphysics. We believe that modeling the birdcage coil in a FEM simulation environment will give more accurate results than the lumped circuit element model of the birdcage coil. The reason is that we have made no assumption while building the FEM models of birdcage coils, whereas lumped element modeling techniques make several assumptions which are mentioned in the previous section. Using these FEM models of the birdcage coil, we have developed a new method to calculate the necessary capacitance value for the birdcage coil. In this method, we have performed an optimization in which the magnitude of the port impedance of the birdcage coil or the variance of the rotating magnetic field inside the coil is used as an objective function and the

capacitance value is used as the control variable. Our goal is to find the optimum capacitance value which maximizes (or minimizes) the objective function.

In addition to capacitance calculation, we have made an eigenfrequency analysis of a birdcage coil using the FEM models of the birdcage coil to calculate the resonant modes of the coil accurately. This analysis provides calculation of not only the resonant modes of the birdcage coil but also any electromagnetic field or variable distributions inside the coil at these resonant modes. Additionally, calculating the resonant modes of a birdcage coil gives an information about the resonance behavior of the coil and using this information tuning and matching procedures of the birdcage coil can be made without interfering with the other modes. On the other hand, to the best of our knowledge, FEM based eigenfrequency analysis of a birdcage coil is also a new study in the field of MRI.

Furthermore, we have performed a frequency domain analysis of a birdcage coil using the same FEM models of the coil. This analysis is used to solve for the electromagnetic fields of a birdcage coil for the given frequency (or frequencies) and capacitance. In other words, this is the basic electromagnetic field solution for a birdcage coil which we have mentioned in previous section and from now on we use the terminology of COMSOL Multiphysics and use the term "frequency domain analysis" often. By making this analysis, one can observe any electromagnetic field distribution inside the coil, for example, B_1 field distribution at the given frequency range, or one can calculate the SAR values at any object inside the coil. We believe that this analysis has significant importance in terms of providing an accurate information about B_1 magnitude (or phase) images to the researchers before they make an actual MR experiment.

In order to make all these design and simulation calculations of low-pass and high-pass birdcage coils according to the user-specified parameters easily, we have developed two software tools using MATLAB (The Mathworks, Natick, USA), which have also a user-friendly graphical user interface (GUI) and connects to COMSOL Multiphysics server to make the FEM based electromagnetic analyses. One of the developed software tools is used to calculate necessary capacitance value and the other software tool is used to make frequency domain analysis and

eigenfrequency analysis of a birdcage coil by performing the proposed methods. We believe that developed software tools have many advantages for the coil designers and the researchers in the field of MRI. First, they can use the tool to calculate the necessary capacitance value for the specified coil dimensions using lumped circuit element model or FEM based optimization method. Second, they may use the tool to find the resonant modes of the coil and electromagnetic field distributions at these resonant modes for any capacitance value using eigenfrequency analysis. Last but not least, they can use the tool to find any electromagnetic field distribution in the volume of interest for both loaded or unloaded birdcage coils. Besides, they can select the excitation type (linear or quadrature excitation) from the tool in the frequency domain analysis so that linearly or circularly polarized B_1 field distributions inside the coil can be obtained easily. Furthermore, users can investigate the SAR at any object inside the coil or other electromagnetic field variables such as induced current in any object by using this software tool.

In order to show that the results of the proposed methods are more accurate than the results of the methods that use lumped circuit element model, we have constructed two handmade birdcage coils (low-pass and high-pass). Using these coils, we have made measurements for different capacitance values and compared the results of the methods with the experimental results.

1.4 Organization of the Thesis

This thesis consists of six chapters. In Chapter 2, analysis of a birdcage coil using lumped circuit element model is presented in details. Methods for calculating the capacitance value and resonance frequency modes are explained in this chapter. Chapter 3 discusses the analysis of a birdcage coil using FEM based simulations. After giving information on building FEM models of birdcage coils, three different electromagnetic analyses of birdcage coils are explained. Then, developed software tools for designing and simulating birdcage coils are presented in Chapter 4. Experimental results are given in Chapter 5. In this chapter, the

results of lumped circuit element model and the results of FEM based simulation methods are compared with the experimental results. Finally, Chapter 6 provides conclusions to the thesis.

Chapter 2

ANALYSIS OF A BIRDCAGE COIL USING LUMPED CIRCUIT ELEMENT MODEL

In this chapter, methods for calculating the necessary capacitance value and the resonance modes of low-pass and high-pass birdcage coils using lumped circuit element model are explained in detail. For the capacitance calculations at given resonance frequency, method presented in [5] is discussed, whereas for the resonant mode calculations, method proposed in [9] is discussed. The reason for choosing these methods among the other methods presented in the literature is that their implementations are easier and results are more in accordance with the experimental results for the frequencies where $\lambda >> coil\ \ dimensions$.

2.1 Capacitance Calculations

In this method, the idea is to calculate the necessary capacitance value from the known current distribution in the rungs and end rings at the given resonance frequency. As previously mentioned, currents in the rungs are proportional to $sin\theta$ (or $cos\theta$) at the resonance frequency. Therefore, current distributions in the end

rings can be easily found since the currents in the rungs are known. These current intensities, then, are used to find the total inductance of each conductor. After finding the total inductance for each rungs and end rings, necessary capacitance value is calculated solving the lumped circuit element model using Kirchhoff's voltage and current law.

As mentioned earlier, in lumped circuit element model, rungs and end rings that are constructed by using copper tube or strip elements are modeled as an inductor. Equivalent lumped circuits for one closed loop of a low-pass and a high-pass birdcage coil are illustrated in Figure 2.1.

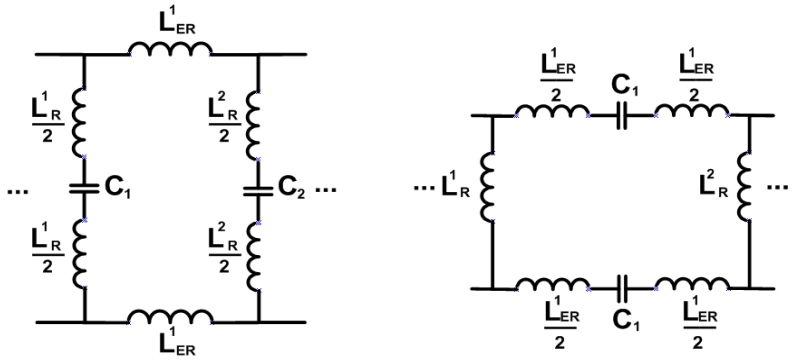

Figure 2.1: Equivalent lumped circuit model for one closed loop of a low-pass birdcage coil (left) and a high-pass birdcage coil (right)

L^i_{ER} and L^i_R in Figure 2.1 are the total inductance of i^{th} end ring and rung respectively. Definition of the total inductance is the combination of self inductance and mutual inductance of a conductor and found by dividing the total magnetic flux linkage of the conductor to the current that flows through in that conductor. It can be alternatively called as effective inductance [5]. In order to better understand the total inductance concept, we can think of a simple example with three conductors parallel to each other in the same plane and three currents flowing through these conductors in the same direction. Total magnetic flux linkage for each conductor can be written as

$$\phi_1 = L_1 I_1 + M_{12} I_2 + M_{13} I_3 \tag{2.1}$$

$$\phi_2 = L_2 I_2 + M_{21} I_1 + M_{23} I_3 \tag{2.2}$$

$$\phi_3 = L_3 I_3 + M_{31} I_1 + M_{32} I_2 \tag{2.3}$$

where ϕ_i is the total magnetic flux linkage of i^{th} conductor, L_i is the self inductance of i^{th} conductor, I_i is the current flows in i^{th} conductor and M_{ij} is the mutual inductance between i^{th} and j^{th} conductors.

Using the definition of total inductance given in previous paragraph, one can express the total inductance of each conductor as

$$\frac{\phi_1}{I_1} = L_1 + M_{12}\frac{I_2}{I_1} + M_{13}\frac{I_3}{I_1} \tag{2.4}$$

$$\frac{\phi_2}{I_2} = L_2 + M_{21}\frac{I_1}{I_2} + M_{23}\frac{I_3}{I_2} \tag{2.5}$$

$$\frac{\phi_3}{I_3} = L_3 + M_{31}\frac{I_1}{I_3} + M_{32}\frac{I_2}{I_3} \tag{2.6}$$

If we generalize the equations given in 2.4 to 2.6 for a coil having a number of K conducting elements, the total inductance of i^{th} conductor can be written as

$$L_X^i = L_i + \beta \sum_{j=1, j\neq i}^{j=K} \frac{I_j}{I_i} M_{ij} \tag{2.7}$$

where subscript X can be either ER (end ring) or R (rung) same as in Figure 2.1, i and j are the indices for the conductors ranging from 1 to K, L_i is the self inductance of i^{th} conductor, M_{ij} is the mutual inductance between i^{th} and j^{th} conductors, I_i and I_j are the known currents flow in i^{th} and j^{th} conductors respectively and β takes a value -1, 0, or 1 according to the direction of the currents in the i^{th} and j^{th} conductors. It can be expressed as

$$\beta = \begin{cases} -1 & \text{if the currents in } i^{th} \text{ and } j^{th} \text{ conductors are in opposite direction} \\ 0 & \text{if } i^{th} \text{ and } j^{th} \text{ conductors are perpendicular to each other} \\ 1 & \text{if the currents in } i^{th} \text{ and } j^{th} \text{ conductors are in same direction} \end{cases} \tag{2.8}$$

After finding the total inductance for each end ring and rung elements of the birdcage coil, necessary capacitance value for the given resonance frequency is calculated. Therefore, calculation of the total inductances based on the calculation of the self inductance, mutual inductance and current distributions of rungs and end rings is the key factor of this method.

2.1.1 Inductance Calculations

In order to calculate the total inductance of a conductor, we need to first calculate the self inductance and mutual inductance of that conductor. Almost every self inductance and mutual inductance calculations presented in the literature are based on the formulas given in [14]. For the formulas will be given in this section, the unit of calculated inductance is in nH and the unit of length parameters are in cm.

2.1.1.1 Self Inductance Calculations

Rungs and end rings are generally constructed using copper tube or strip. According to the cross section of these elements illustrated in Figure 2.2, there are two different formulas used in self inductance calculations.

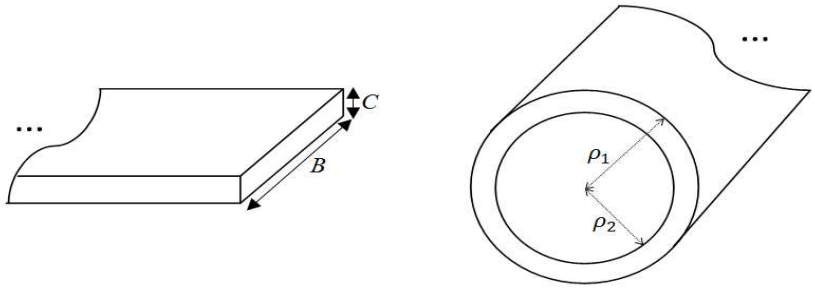

Figure 2.2: Illustration of the conductors which have rectangular cross-section (left) and annular cross-section (right)

For the rungs and end rings, which have rectangular cross section, self inductance is calculated from the formula given as

$$L = 0.002l \left[\ln\left(\frac{2l}{B+C}\right) + 0.5 - \ln\epsilon \right] \tag{2.9}$$

where B is the width, C is the thickness of a conductor shown in Figure 2.2, l is the length of a conductor, and $\ln\epsilon$ can be found from the table in [14] according to the $\frac{C}{B}$ ratio. For our case, since $C << B$, the ratio of $\frac{C}{B}$ is approximately 0 and using this ratio, $\ln\epsilon$ is found as 0 from the table in [14]. Therefore, Equation

2.9 can be simplified as

$$L = 0.002l \left[\ln\left(\frac{2l}{B}\right) + 0.5 \right] \tag{2.10}$$

For the rungs and end rings, which is constructed using copper tube, the formula of the self inductance is written as

$$L = 0.002l \left[\ln\left(\frac{2l}{\rho_1}\right) + \ln\zeta - 1 \right] \tag{2.11}$$

where ρ_1 and ρ_2 are the outer and inner radii of the cross section of a tubular conductor shown in Figure 2.2, l is the length of a conductor, and $\ln\zeta$ can be found according to the $\frac{\rho_2}{\rho_1}$ ratio from the table in [14]. Since the thickness of the copper is very small, ρ_1 and ρ_2 are approximately equal to each other and according to the ratio $\frac{\rho_2}{\rho_1} \approx 1$, $\ln\zeta$ is read as 0 from the table in [14]. Therefore, Equation 2.11 can be rewritten as

$$L = 0.002l \left[\ln\left(\frac{2l}{\rho_1}\right) - 1 \right] \tag{2.12}$$

2.1.1.2 Mutual Inductance Calculations

Calculations of the mutual inductance between coil elements are more complicated than calculations of the self inductance. For the unshielded birdcage coils, mutual inductances calculations can be divided into two categories: mutual inductance between the rungs and end ring segments. In shielded birdcage coils, on the other hand, mutual inductance between RF shield and rungs, end rings segments and RF shield must be also taken into consideration. Since rungs and end rings are geometrically perpendicular to each other, mutual inductance between them will be 0.

Using the formulas given in [14], mutual inductance between two rungs can be thought as mutual inductance between two equal parallel straight filaments and calculated using the formula given as

$$M = 0.002l \left[\ln\left(\frac{l}{d} + \sqrt{1 + \frac{l^2}{d^2}}\right) - \sqrt{1 + \frac{d^2}{l^2}} + \frac{d}{l} \right] \tag{2.13}$$

where l is the length of the rung and d is the perpendicular distance between two rungs.

For the mutual inductance calculations between end ring segments, different formulas proposed in the literature can be used. One of the methods recommended in [3] is to use Neumann formula which can be found in [14]. The other method presented in [5] is to use the formula for mutual inductance calculations for non-parallel element in the same plane given in [14]. In this method, end rings are split into equal segment vectors whose directions are defined by the currents flow in that segments. Segmentation of 8-leg birdcage coil is illustrated in Figure 2.3.

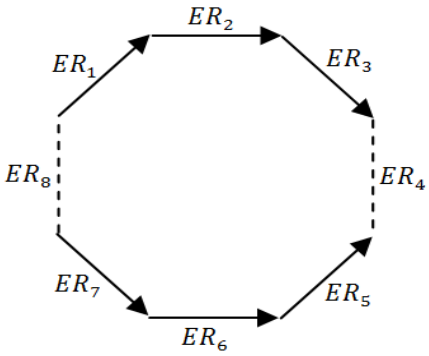

Figure 2.3: Illustration of end ring segments for 8-leg birdcage coil

At the resonance frequency, current directions in one of the end rings are shown in Figure 2.3. Since there is no current flow in ER_8 and ER_4 segments, they are drawn with dashed lines.

In order to find the mutual inductance between two end ring segments, following formula given in [14] is used.

$$M = 0.002\cos(\theta)[(\mu + l)\tanh^{-1}\left(\frac{m}{R_1+R_2}\right) + (v+m)\tanh^{-1}\left(\frac{l}{R_1+R_4}\right) - \mu\tanh^{-1}\left(\frac{m}{R_3+R_4}\right) - v\tanh^{-1}\left(\frac{l}{R_2+R_3}\right)] \tag{2.14}$$

Here in Equation 2.14, l and m are the lengths of two end ring segments, μ and v are the distances from the intersection point of the end rings to their nearer ends and R_1,R_2,R_3, and R_4 are the distances between tip of the end rings, and θ

is the angle between end rings. These parameters shown in Figure 2.4 are given in the following equations.

$$2\cos(\theta) = \frac{\alpha^2}{lm}, \;\; where \;\; \alpha^2 = R_4^2 - R_3^2 + R_2^2 - R_1^2 \tag{2.15}$$

$$\mu = \frac{\left[2m^2\left(R_2^2 - R_3^2 - l^2\right) + \alpha^2\left(R_4^2 - R_3^2 - m^2\right)\right] l}{4l^2m^2 - \alpha^4} \tag{2.16}$$

$$v = \frac{\left[2l^2\left(R_4^2 - R_3^2 - m^2\right) + \alpha^2\left(R_2^2 - R_3^2 - l^2\right)\right] m}{4l^2m^2 - \alpha^4} \tag{2.17}$$

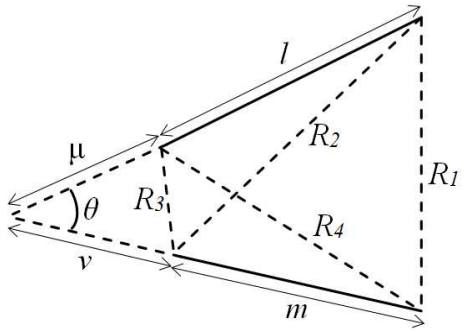

Figure 2.4: Schematic drawing for mutual inductance calculation between two conductive elements in the same plane

As shown in Figure 2.4, these formulas are given for two conductive elements with unequal lengths in the same plane. Since the length of end ring segments are equal, we can use above formulas by taking $m = l$. For the mutual inductance between adjacent end ring segments, *e.g.*, ER_2 and ER_3 in Figure 2.2, μ and v must be taken as 0 in Equation 2.14. For the mutual inductance between parallel end ring segments, *e.g.*, ER_1 and ER_5 in Figure 2.2, Equation 2.13 must be used.

After finding the self inductances and mutual inductances for each rung and end ring segment, one can calculate the total inductance for these elements using the formula given in Equation 2.7 and then, find the necessary capacitance value by solving the lumped circuit element model for low-pass and high-pass birdcage coil.

2.1.2 Capacitance Calculation for Low-Pass Birdcage Coil

In order to calculate the necessary capacitance value for the low-pass birdcage coil, equivalent circuit given in Figure 2.5 need to be solved using Kirchhoff's voltage and current law.

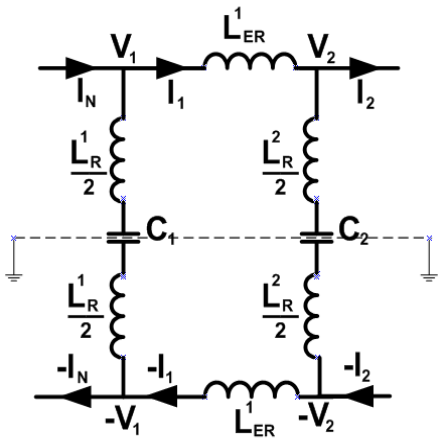

Figure 2.5: Equivalent lumped circuit element model for N-leg low-pass birdcage coil with virtual ground, voltages and currents

Here in Figure 2.5, midpoint of the capacitors are treated as virtual ground to simplify the calculations. First, we can write the voltage difference across the ER_1 segment as

$$V_1 - V_2 = jwL^1_{ER}I_1 \tag{2.18}$$

where $w = 2\pi f_{res}$ and f_{res} is desired resonance frequency. Then, V_1 and V_2 can be written as in Equation 2.19 and 2.20 respectively by taking the virtual ground as reference point.

$$V_1 = (I_N - I_1)\left(\frac{jwL^1_R + (jwC_1)^{-1}}{2}\right) \tag{2.19}$$

$$V_2 = (I_1 - I_2)\left(\frac{jwL^2_R + (jwC_2)^{-1}}{2}\right) \tag{2.20}$$

In circular birdcage coil design, capacitances of the capacitors on the rungs or end rings must be same in order to obtain circularly polarized B_1 field inside the coil. Additionally, total inductance of the rungs or end ring segments are also the same, since they are identical. Therefore, we can simplify the equations by

writing C for the capacitance values, L_R for the total inductance of the rungs and L_{ER} for the total inductance of the end rings as given in Equation 2.21.

$$\begin{aligned} C_1 = C_2 = ... = C_N = C \\ L_R^1 = L_R^2 = ... = L_R^N = L_R \\ L_{ER}^1 = L_{ER}^2 = ... = L_{ER}^N = L_{ER} \end{aligned} \tag{2.21}$$

At last, substituting V_1 and V_2 in Equation 2.19 and 2.20 into the Equation 2.18, the formula of the necessary capacitance value for given resonance frequency is obtained as

$$C = \frac{I_N - 2I_1 + I_2}{w^2 L_R (I_N - 2I_1 + I_2) - 2w^2 L_{ER} I_1} \tag{2.22}$$

If we generalize the Equation 2.22, necessary capacitance value can be found (using the currents in any adjacent three end ring segments) from the formula given as

$$C = \frac{I_{i-1} - 2I_i + I_{i+1}}{w^2 L_R (I_{i-1} - 2I_i + I_{i+1}) - 2w^2 L_{ER} I_i} \tag{2.23}$$

2.1.3 Capacitance Calculation for High-Pass Birdcage Coil

Calculation of the capacitance for high-pass birdcage coil is achieved by using the same approach for low-pass birdcage coil expressed in previous section. Equivalent lumped circuit model for the high-pass birdcage coil is illustrated in Figure 2.6.

First, we can write the voltage difference $(V_1 - V_2)$ across the ER_1 segment as

$$V_1 - V_2 = (jwL_{ER}^1 + (jwC_1)^{-1})I_1 \tag{2.24}$$

Then, we can write V_1 and V_2 as in Equation 2.25 and 2.26 respectively. Since the midpoints of the rungs are treated as virtual ground, only half of the total

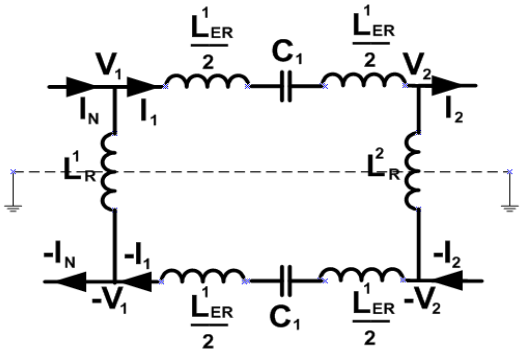

Figure 2.6: Equivalent lumped circuit element model for N-leg high-pass birdcage coil with virtual ground, voltages and currents

inductance of the rungs is taken into consideration.

$$V_1 = (I_N - I_1)\left(\frac{jwL_R^1}{2}\right) \tag{2.25}$$

$$V_2 = (I_1 - I_2)\left(\frac{jwL_R^2}{2}\right) \tag{2.26}$$

By substituting Equations 2.25 and 2.26 into Equation 2.24 and using the equality given in Equation 2.21, generalized formula of the necessary capacitance value for the high-pass birdcage coil can be written as

$$C = \frac{2I_i}{w^2 L_{ER} 2I_i - w^2 L_R(I_{i-1} - 2I_i + I_{i+1})} \tag{2.27}$$

2.2 Resonant Modes Calculations

In this method, the idea is to find the resonant modes (or frequencies) of a birdcage coil for given coil dimensions and capacitances by solving the generalized eigenvalue value problem given as

$$A\mathbf{v} = \lambda B\mathbf{v} \tag{2.28}$$

where A and B are $N \times N$ matrices, values of $\mathbf{v}$ are the generalized eigenvectors and the values of λ are the generalized eigenvalues that satisfy the Equation 2.28.

In previous method, since we were only interested in $m = 1$ resonant mode,

current distributions in the rungs were known parameters. In this method, however, we aim to find all resonant modes and each of them has different current distributions. Therefore, currents in the conductive elements must be unknown parameters in order to find the all resonant modes of a birdcage coil. Furthermore, in previous method, we introduced the total inductance concept and it was the basis of capacitance calculations. However, in this method, since currents are unknown parameters we cannot use the formula of total inductance given in Equation 2.7. For this reason, we can use mesh current method and write an equation for any loop using self and mutual inductances found in previous section and unknown mesh currents shown in Figure 2.7.

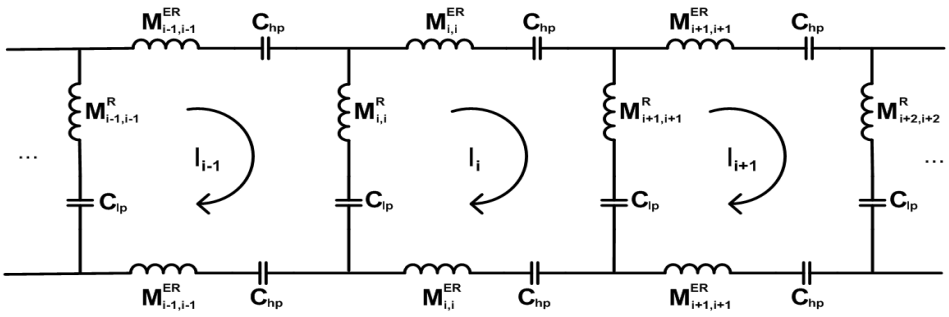

Figure 2.7: Equivalent lumped circuit element model for N-leg hybrid (high-pass and low-pass) birdcage coil with mesh currents. For the high-pass birdcage coil design $C_{lp} = 0$, and for the low-pass birdcage coil design $C_{hp} = 0$.

Notation used in Figure 2.7 is different than the previous notations. Here, $M^R_{i,i}$ and $M^{ER}_{i,i}$ are the self inductance of the rungs and end rings respectively. $M^R_{i,k}$ where $i \neq k$, is the mutual inductance between i^{th} and k^{th} rungs and similarly, $M^{ER}_{i,k}$ where $i \neq k$, is the mutual inductance between i^{th} and k^{th} end rings. I_i is the current flows in the i^{th} mesh.

For N-leg high-pass birdcage coil design (where $C_{lp} = 0$ in Figure 2.7), according to Kirchoff's voltage law, we can write an equation for the i^{th} mesh as

$$jw\left(\sum_{k=1}^{N} M^R_{i,k}(I_k - I_{k-1}) + \sum_{k=1}^{N} M^R_{i+1,k}(I_{k-1} - I_k) + \sum_{k=1}^{N} 2M^{ER}_{i,k} I_k\right) = \frac{2j}{wC_{hp}} I_i \tag{2.29}$$

where $i = 1, 2, ..., N$. Leaving the mesh currents alone and taking $\lambda = 1/w^2$,

Equation 2.29 can be rewritten as

$$\sum_{k=1}^{N} \left(M_{i,k}^{R} - M_{i+1,k}^{R}\right) I_k - \sum_{k=1}^{N} \left(M_{i,k}^{R} - M_{i+1,k}^{R}\right) I_{k-1} + \sum_{k=1}^{N} 2M_{i,k}^{ER} I_k = \frac{2\lambda}{C_{hp}} I_i \quad (2.30)$$

In order to write Equation 2.30 in the form of generalized eigenvalue problem given in Equation 2.28, we can rewrite Equation 2.30 as

$$\sum_{k=1}^{N} \left(M_{i,k}^{R} - M_{i+1,k}^{R}\right) I_k - \sum_{k=0}^{N-1} \left(M_{i,k+1}^{R} - M_{i+1,k+1}^{R}\right) I_k + \sum_{k=1}^{N} 2M_{i,k}^{ER} I_k = \frac{2\lambda}{C_{hp}} I_i \quad (2.31)$$

Since the term $k = 0$ can be interpreted as $k = N$, we can now write Equation 2.31 in the form of Equation 2.28 as

$$A\mathbf{I} = \lambda B\mathbf{I} \quad (2.32)$$

where

$$\begin{aligned} \mathbf{I} &= [I_1, I_2, ..., I_N]^T \\ A_{i,k} &= M_{i,k}^{R} - M_{i+1,k}^{R} - M_{i,k+1}^{R} + M_{i+1,k+1}^{R} + 2M_{i,k}^{ER} \\ B &= I_d^{N\times N}\left(\frac{2}{C_{hp}}\right), \ where \ I_d^{N\times N} : Identity \ matrix \end{aligned} \quad (2.33)$$

Since self and mutual inductances can be calculated using the formulas explained in previous section, non-trivial solutions of Equation 2.32 can be found by solving the determinant equation given as

$$det[A - \lambda B] = 0 \quad (2.34)$$

There are N number of solutions $(\lambda_1, \lambda_2, ..., \lambda_N)$ of Equation 2.34. Using these eigenvalues, one can find the resonant modes of high-pass birdcage coil from the formula $\lambda = 1/w^2$.

In order to find the resonant modes of N-leg low-pass birdcage coil design (where $C_{hp} = 0$ in Figure 2.7), similar approach used in high-pass birdcage coil is applied to the circuit model illustrated in Figure 2.7. In the end, we come up

with the same equation given in 2.32. Matrix A in this equation is the same as in Equation 2.33, whereas matrix B is different and expressed as

$$\begin{aligned} B_{i,k} &= -\frac{1}{C_{lp}} \qquad for \quad k = i-1, \\ B_{i,k} &= \frac{2}{C_{lp}} \qquad for \quad k = i, \\ B_{i,k} &= -\frac{1}{C_{lp}} \qquad for \quad k = i+1, \\ B_{i,k} &= 0 \qquad for\ other\ k. \end{aligned} \tag{2.35}$$

Then, one can find the resonant modes of low-pass birdcage coil by putting A and B matrices in Equation 2.34 and solving this equation.

2.3 Discussion and Conclusion

In this chapter, methods of calculation of capacitances and resonant modes of low-pass and high-pass birdcage coils using lumped circuit element model are discussed and closed-form expressions for both capacitance and resonant mode calculations are given explicitly. These methods are very useful for the coil designers in terms of knowing the initial capacitance value and frequency spectrum of the coil before tuning and matching process. It is important to note that these calculations are given for unshielded birdcage coil design. However, analysis of shielded birdcage coil design can be found in [9].

In given capacitance calculation method, only the dominant frequency mode ($m = 1$) is considered. Therefore, since the current distribution in the rungs at this frequency is well known, currents in the end rings can be easily found. These known current distributions is the starting point of this method. Second point is the calculation of the inductances of the rungs and end rings. These calculations are made using the handbook formulas based on the coil geometry. Then, total inductance (or effective inductance) concept based on the known current distributions and inductances is introduced. If we know the total inductance of each element of a birdcage coil, we can calculate the necessary capacitance value for

given desired frequency by solving the simple circuit equations.

In given resonant mode calculation method, on the other hand, we are interested in all resonant modes of the birdcage coil. Therefore, we cannot use the sinusoidal current distribution for all resonant modes. We need to take these current distributions as unknown parameters and solve a generalized eigenvalue problem in which the eigenvectors correspond to the mesh currents and eigenvalues are related with the resonant modes of the birdcage coil with a simple formula. In addition to calculation of the resonant modes, one can calculate the mesh currents for each eigenvalue in order to calculate the B_1 field for each mode using Biot-Savart law.

Although given methods are easy to implement and have a good accuracy in the calculation of capacitance and resonant modes of the birdcage coil, they have some limitations. First of all, calculations given for both methods heavily depend on the inductance calculations which are based on only the coil geometry and independent of the frequency. As the frequency increases, accuracy of the calculated inductances as well as the calculated capacitance and resonant modes will decrease. Second, inductance calculations are based on some assumptions. For example, when calculating the mutual inductance between end ring segments, they are modeled as a straight element instead of circular element. It can be suitable for the birdcage coil whose end ring segments are very small and can be modeled as straight element, but the accuracy of calculating capacitance and resonant modes will decrease as the length of end ring segments increases (or number of rungs decreases). Last but not least, modeling a birdcage coil with calculated capacitance value in a simulation environment and making electromagnetic analysis inside the coil is as important as practically designing a birdcage coil. These electromagnetic analyses provide not only necessary capacitance value or resonant modes accurately but also complete analysis of the birdcage coil such as any electromagnetic variable distributions inside the loaded (or unload) and shielded or (unshielded) coil. In the next section, complete analysis of birdcage coils using FEM based simulation methods will be presented.

Chapter 3

ANALYSIS OF A BIRDCAGE COIL USING FEM BASED SIMULATIONS

In this chapter, detailed analyses of low-pass and high-pass birdcage coils using the 3D simulation of FEM models developed in COMSOL Multiphysics are presented. In the first section of this chapter, these models are explained with respect to all aspects of FEM: geometry, physics, boundary condition and mesh. Then, three different electromagnetic analyses, which are made using the FEM models of low-pass and high-pass birdcage coils, are discussed in Section 3.2. These are frequency domain analysis which is basically the electromagnetic field solution of a birdcage coils at a given frequency, capacitance calculation using FEM based optimization which is the new method to calculate the necessary capacitance value for the birdcage coils and eigenfrequency analysis used in order to calculate the resonant modes of birdcage coils.

3.1 FEM Models of Birdcage Coils

In this section, low-pass and high-pass birdcage coil models developed in COMSOL Multiphysics are discussed. We first start with the geometry of these models. As given in Figure 1.2 in the first chapter, capacitors in low-pass birdcage coil are placed on the rungs whereas in high-pass birdcage coils they are placed on the end-rings. With this capacitor placement, birdcage coils are first geometrically modeled in the simulation environment as shown in Figure 3.1.

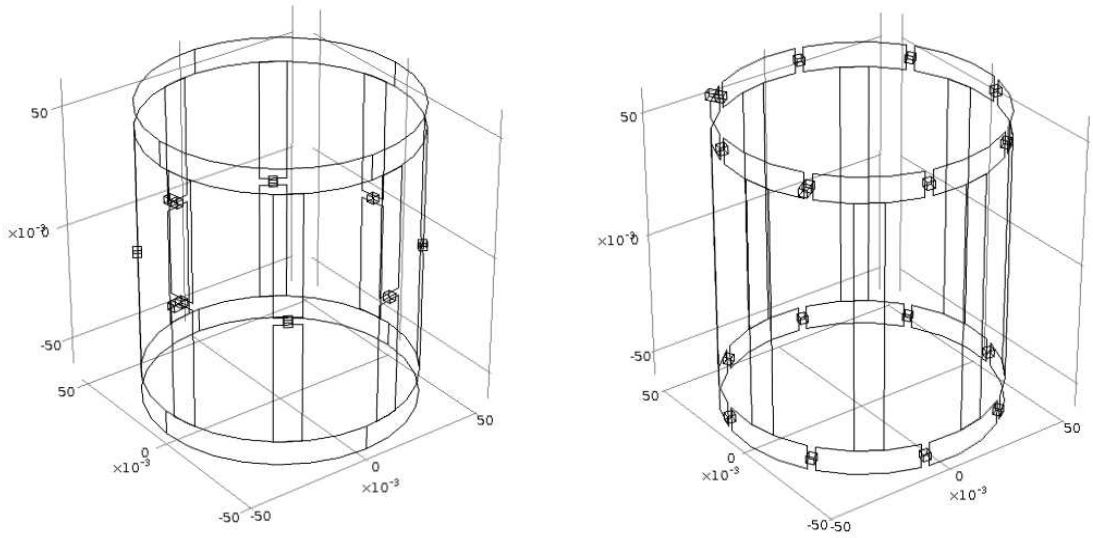

Figure 3.1: Low-pass (left) and high-pass (right) birdcage coil geometric models

As given in Figure 3.1, rungs and end-rings are modeled as rectangular strips without thickness and lumped capacitors are modeled as parallel plate capacitors. Capacitance value is set by altering the relative permittivity (ϵ_r) of the material assigned to the capacitors using the formula

$$C = \epsilon_0 \epsilon_r \frac{A}{d} \tag{3.1}$$

where ϵ_0 is the permittivity of free space, A is the area of parallel plates and d is the distance between the parallel plates.

After modeling the geometry of the coils, *Electromagnetic Waves* interface is added under the *Radio Frequency* branch for the physics selection of the model.

This interface solves the electromagnetic wave equation for time harmonic and eigenfrequency problems and the equation is given as

$$\nabla \times \mu_r^{-1}(\nabla \times \mathbf{E}) - k_0^2 \left(\epsilon_r - \frac{j\sigma}{\omega \epsilon_0} \right) \mathbf{E} = 0 \tag{3.2}$$

where $\mathbf{E}$ is the electric field vector, μ_r is the relative permeability, σ is the conductivity and k_0 is the wave number of free space and is expressed as

$$k_0 = \omega \sqrt{\epsilon_0 \mu_0} \tag{3.3}$$

After adding physics for the model, we now need to assign boundary conditions to the surfaces of coil elements as well as the outer boundary of the solution domain enclosing the coil geometry. Since the thickness of the copper strip used to construct birdcage coils is larger than the skin-depth at the frequencies we are interested in, Perfect Electric Conductors (PEC) is assigned to the rungs and end-rings boundaries. By assigning this boundary condition, we set the tangential component of electric field of these boundaries to zero ($\mathbf{n} \times \mathbf{E} = 0$). In addition to rungs and end-rings, capacitor plates and RF shield (if exists) boundaries are also assigned as PEC. PEC boundaries of a low-pass birdcage coil are illustrated in Figure 3.2.

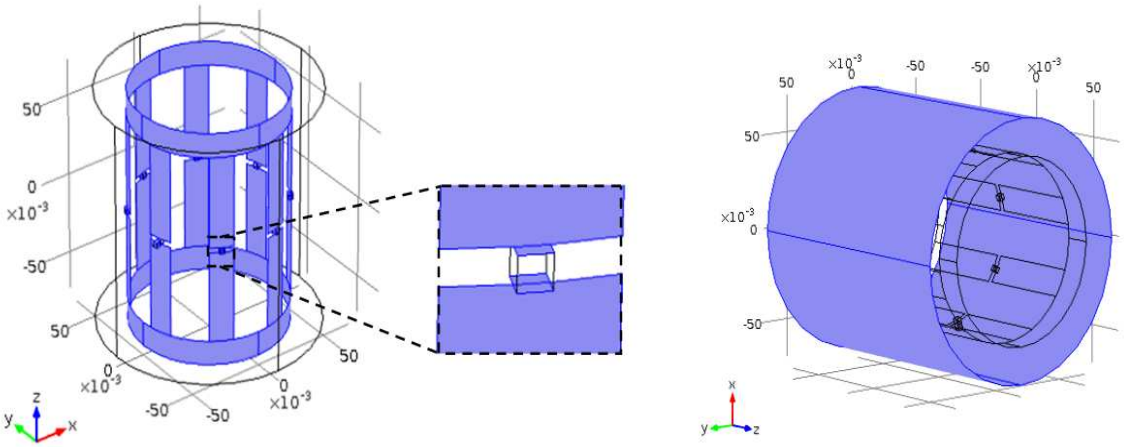

Figure 3.2: PEC boundaries: Rungs, end rings and capacitor plates (left), RF shield (right)

In order to prevent reflections from the outer boundary of the solution domain (sphere) enclosing the coil geometry, scattering boundary condition or perfectly matched layer (PML) is used [15] [16]. Among them, scattering boundary condition is applied to the exterior boundaries and make the specified boundary transparent to outgoing waves. This can be a plane, cylindrical or spherical wave but for our condition it is a spherical wave. PML, on the other hand, is a type of domain feature and is used for simulating an infinite domain in which the wave can propagate and disappear by attenuation without any reflection. In Figure 3.3, boundaries (or layers) of the sphere enclosing the coil geometry are shown.

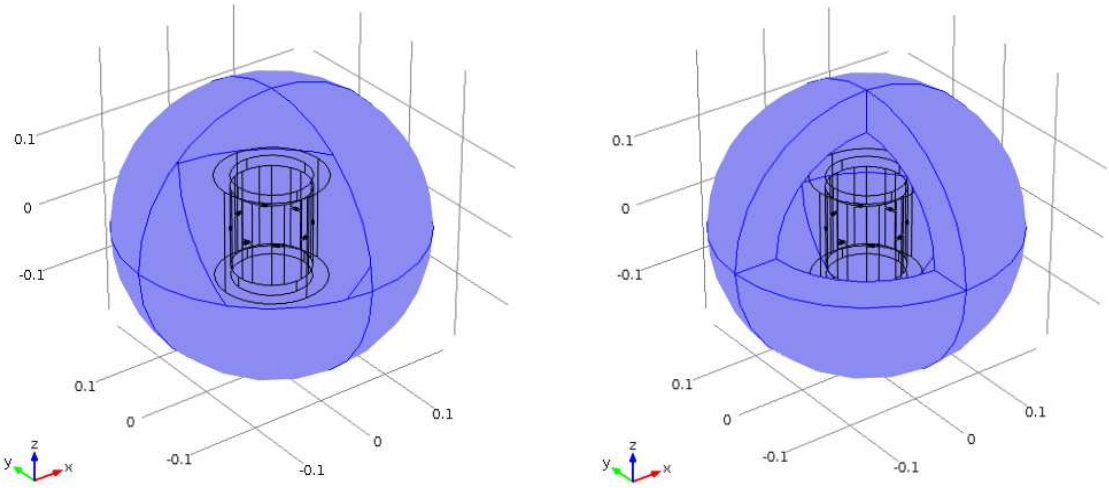

Figure 3.3: Sphere boundaries assigned to a scattering boundary condition (left), sphere layers are defined as PML (right)

At last, in frequency domain analysis, lumped port boundary condition is used for voltage excitation [15]. Equation for lumped port boundary condition is simply given as

$$Z_{port} = \frac{V_{port}}{I_{port}} \tag{3.4}$$

where V_{port} is the excited voltage, I_{port} is the port current, and Z_{port} is the port impedance. It is important to note that while applying lumped port boundary condition, lumped port boundary where the voltage or current is applied must be placed between metallic type boundaries such as PEC. Lumped port boundaries of one-port and two-port excitations models are shown in Figure 3.4.

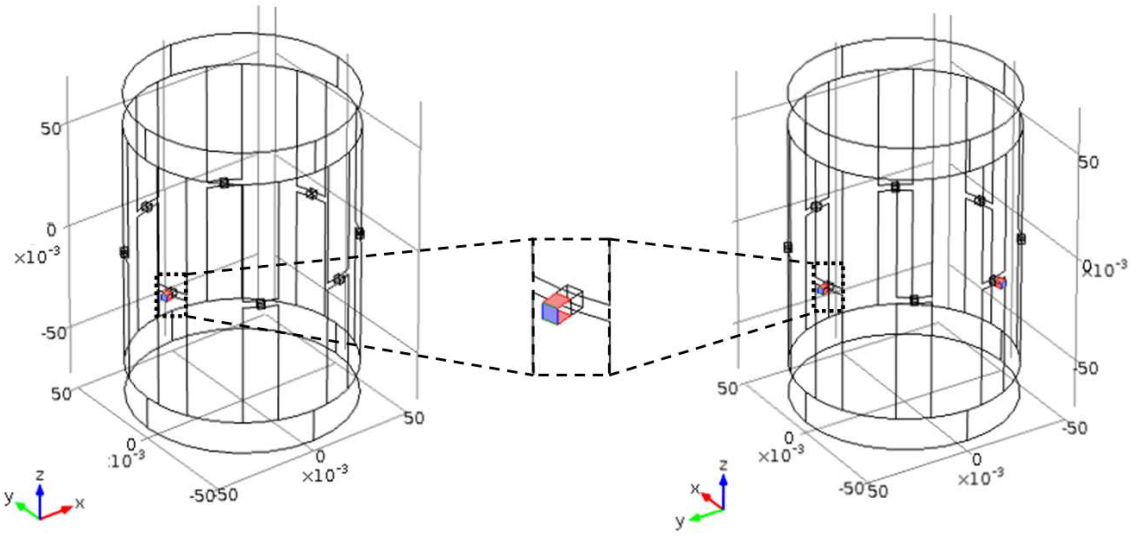

Figure 3.4: One-port excitation model (left), two-port excitation model (right). Lumped port boundaries are shown with purple color, PEC boundaries are shown with red color.

As can be seen in Figure 3.4, voltage is applied from the boundary (shown with purple colour) which is placed between PEC boundaries (shown with red colour) and these PEC boundaries are connected to the corresponding capacitor plates.

After adding physics and boundary conditions, we generate a mesh for the model in order to discretize the complex geometry of the birdcage coil into triangular and tetrahedral elements. It is important that in electromagnetic wave problems, wavelength must be taken into consideration while generating a mesh in order to get accurate results. According to [15], maximum element size of the mesh elements must be at least one fifth of the wavelength at the interested frequency range. Generated mesh of an 8-leg low-pass birdcage model is given as an example in Figure 3.5.

For the final step, we need to add study and solver sequence for the model in order compute the solutions. Since this step is about COMSOL Multiphysics usage, we have decided to explain this step in the following note.

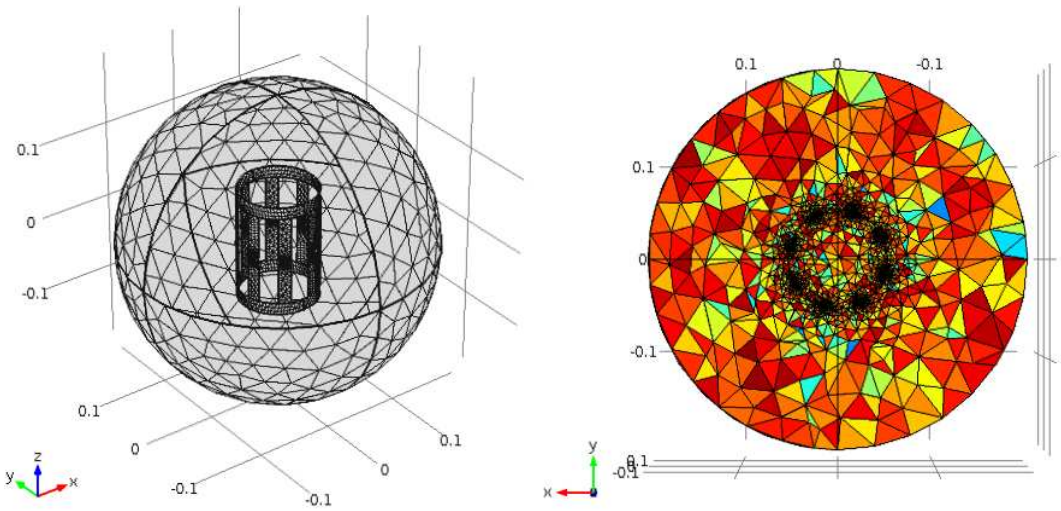

Figure 3.5: Generated mesh at the boundary surfaces of the low-pass birdcage model (left), x-y plane at z=0 (right)

3.1.0.1 Note: Adding study and solver sequence in COMSOL Multiphysics

In COMSOL Multiphysics, there are several study types corresponding to the physics that the user has added. For instance, we have added *Electromagnetic Waves* physics interface under the *RF module*. For this physics interface, we can choose different studies such as *Frequency Domain Study* for solving the wave equation or a frequency response of a model, *Time Dependent Study* for making transient simulations, *Eigenfrequency Study* for finding resonant modes of a model or *Stationary Study* for steady-state analysis of a model. After adding one of the study types, we need to add necessary solver sequence that corresponds to that study such as *Stationary Solver*, *Time-Dependent Solver*, *Eigenvalue solver* or *Optimization Solver*. One can also use the default solver sequence for the corresponding study. For instance, after adding *Frequency Domain Study* and specifying necessary parameters such as frequency range, mesh selection and physics selection, user can solve the model by clicking the *Compute* button. In this case, *Stationary Solver* is automatically added as a solver sequence since it is the default solver of the *Frequency Domain Study*. On the other hand, if we want to make an optimization in our model in *Frequency Domain Study*, in this

case, we need to choose the solver as *Optimization Solver* instead of using default solver. Additionally, user can modify the default value of solver parameters such as relative tolerance which is used for termination of the iterative processes or linearization point which is used in eigenvalue solver and specifies a point around where the solution is linearized. After adding study types and solver sequences, and specifying the necessary parameters from the study and solver settings, we can compute the solution of a birdcage model that we have developed.

3.2 Methods

In this section, three different electromagnetic analyses of developed birdcage coils will be discussed.

3.2.1 Frequency Domain Analysis of a Birdcage Coil

We have first made a frequency domain analysis of the developed birdcage models in COMSOL Multiphysics. As previously mentioned, frequency domain analysis is used to solve for the electromagnetic fields of the birdcage coil at a given frequency (or frequencies) and can be used for several purposes. For instance, it can be used to observe any electromagnetic field variables in the model such as B_1 field distribution inside the coil, surface current density in the rungs or induced currents in the conductive objects. Additionally, one can estimate the SAR values of any object inside the birdcage coil. Last but not least, instead of making the simulations at one frequency, one can specify more than one frequencies where the solution will be computed at, in order to observe the variation of any electromagnetic field parameters with respect to the frequency.

3.2.1.1 Linear and Quadrature Excitation

In frequency domain analysis, we have driven the birdcage coil using two different excitations: linear and quadrature excitation. As mentioned earlier, in linear excitation, birdcage coil is driven from one port (shown in Figure 3.4) that generates a linearly polarized B_1 field inside the coil. This linearly polarized field is the combination of two circularly polarized fields that are left-hand rotating and right-hand rotating fields. Since the effect of right hand rotating field on the spins is negligible, we consider only the left hand rotating field, which is also called excitatory component or positive rotating component of the magnetic field. In quadrature excitation, on the other hand, birdcage coil is driven from two ports (shown in Figure 3.4) that are geometrically 90° apart from each other and driving signals are 90° out of phase that generates a circularly polarized field inside the coil. The advantage of quadrature excitation of birdcage coils has already been mentioned in the first chapter.

If we assume that the main magnetic field is in the negative z-direction, the transmit sensitivity of the coil corresponds to the positively rotating component of the magnetic field (H^+) and the receive sensitivity of the coil corresponds to the negatively rotating component of the magnetic field (H^-) and they can be expressed as [17]

$$\begin{aligned} H^+ &= \frac{H_x + iH_y}{2} \\ H^- &= \frac{(H_x - iH_y)^*}{2} \end{aligned} \tag{3.5}$$

where H_x and H_y are the x and y component of the magnetic field respectively and asterisk indicates the complex conjugate.

3.2.1.2 Study and Solver Sequence

After modeling the low-pass and high-pass birdcage coil as given in Section 3.1, we need to add study and solver sequence for the model in order to compute the solutions. For the frequency domain analysis, we first add *Frequency Domain*

Study as study type and specify the frequency range from the study settings. Then, we choose the *Stationary* node as the solver sequence and select the biconjugate gradient stabilized (BiCGStab) method with a left pre-conditioner as the solver [18]. This method is one of the iterative solvers in COMSOL Multiphysics and is used to solve linear systems of the form $Ax = b$ which is obtained using Equation 3.2 for the *Electromagnetic Waves* interface.

3.2.1.3 Simulation Results

First simulation has been made for unshielded and empty 8-leg low-pass birdcage coil with a diameter of 10 *cm*, rung length of 11.5 *cm*, and rung and end-ring width of 1.5 *cm*. Capacitance value used on the rungs is 10.3 *pF* and the simulation frequency is 123.25 *MHz*. Total number of degrees of freedom in the equation system is about 600000. Computations have been performed on a workstation with 2 Intel Xeon X5675 (3.07GHz) processors and 64GB of memory. Frequency domain analysis of the model takes about 1 minutes for one frequency.

Geometric model of this coil was given in Figure 3.1. We have made both linear and quadrature excitation. Magnitude images of H^+ and H^- at the central slice (z=0) for linear excitation are given in Figure 3.6.

As can be seen in Figure 3.6, left-rotating and right-rotating components of the magnetic fields at the specified frequency are the same in linear excitation case and their combination produces a linearly polarized field inside the coil. On the other hand, when a birdcage coil is driven from two ports (quadrature excitation), H^- should be zero and $H^+ >> H^-$. Magnitude images of H^+ and H^- at the central slice (z=0) for quadrature excitation are given in Figure 3.7.

As illustrated in Figure 3.7, H^+ is uniform especially at the central region of the coil and H^- is almost zero in the same region in the quadrature excitation. This is the ideal case for quadrature birdcage coils. In practice, H^- never equals to zero due to the imperfections in birdcage coil geometry, but H^+ is still very much larger than the H^-.

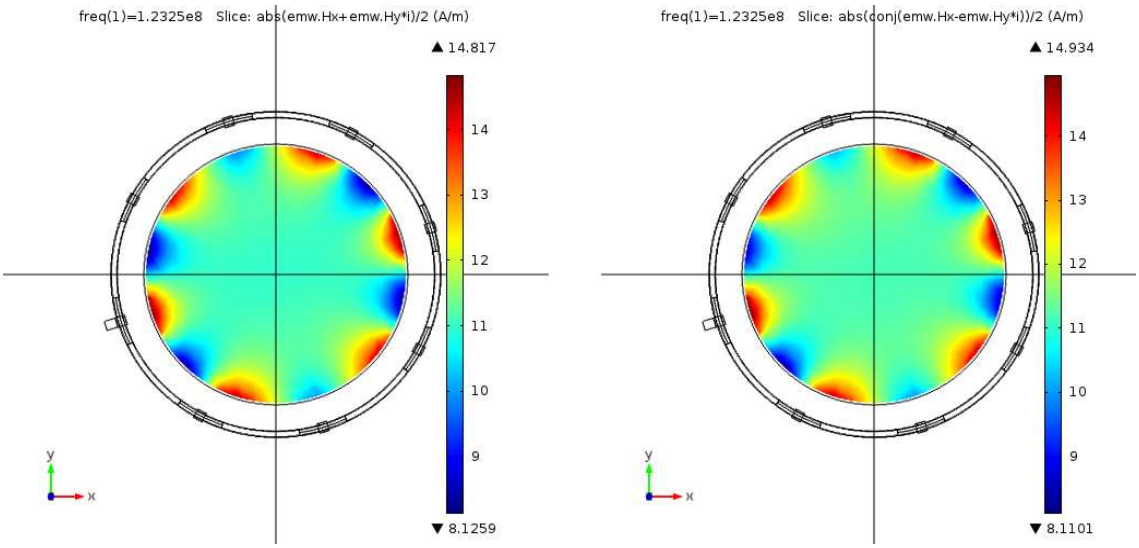

Figure 3.6: Magnitude images of H^+ (left), and H^- (right) at the central slice (z=0) for linear excitation

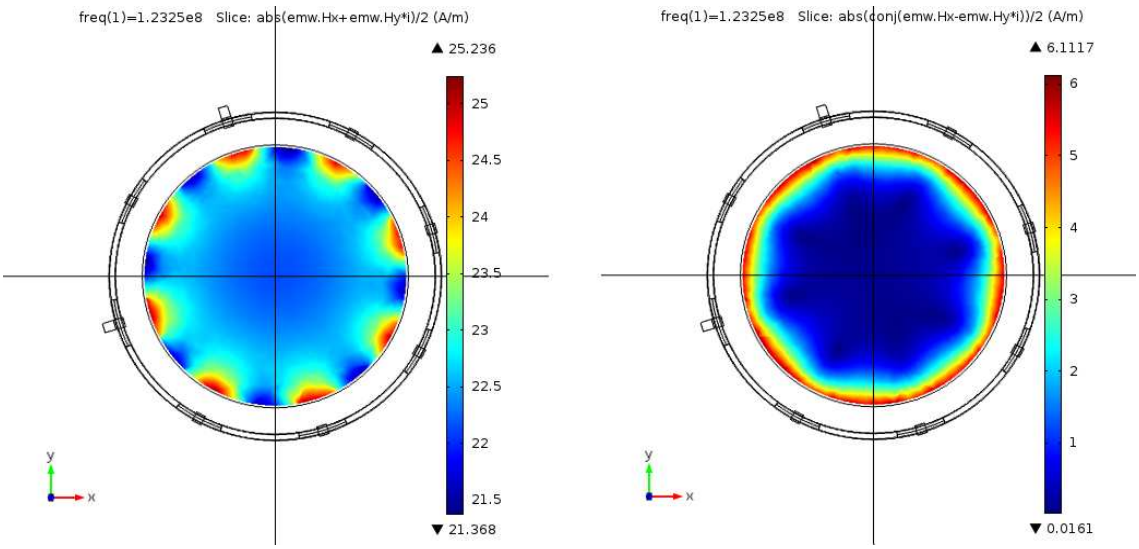

Figure 3.7: Magnitude images of H^+ (left), and H^- (right) at the central slice (z=0) for quadrature excitation

One can also observe the electric field inside the coil for both excitations. Magnitude images of electric field at the central slice (z=0) for both linear and quadrature excitations are illustrated in Figure 3.8.

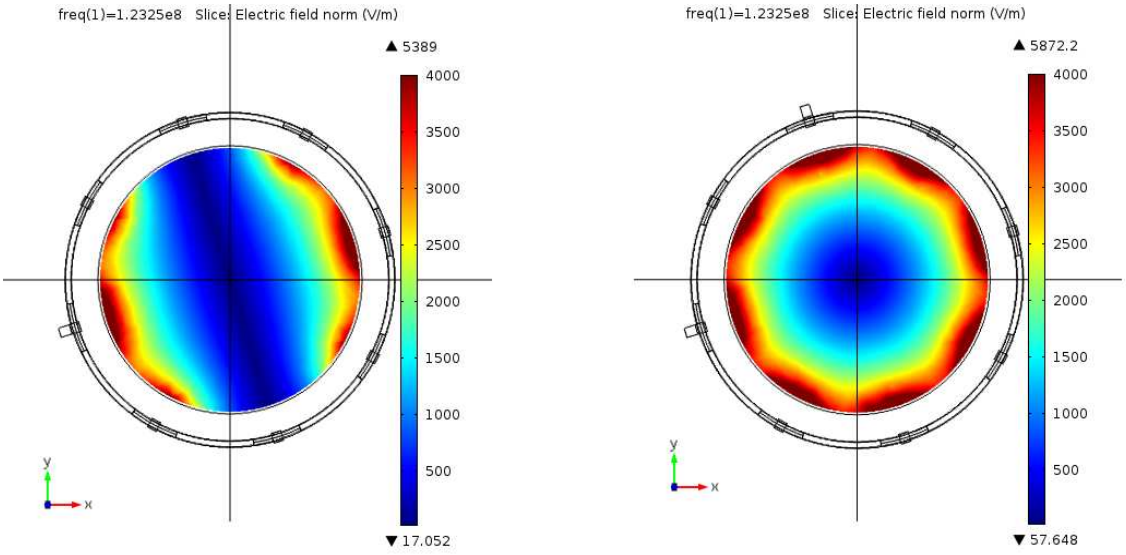

Figure 3.8: Magnitude image of E-field for linear excitation (left), magnitude image of E-field for quadrature excitation (right) at the central slice (z=0)

Apart from the field solutions, we can also observe other electromagnetic variables in the model such as current distribution in the rungs. We know that currents in the rungs have sinusoidal distribution at the desired frequency. In Figure 3.9, z-component of the surface current densities in the rungs are illustrated with the surface arrow plot.

Second simulation has been made for empty and shielded 8-leg low-pass birdcage coil with a shield diameter of 14 *cm*, shield length of 14.5 *cm* and the rest are the same with the dimensions used in the first simulation. Used capacitance value is 14.2 *pF* and the simulation frequency is 123.25 *MHz*. Model geometry for shielded birdcage coil was illustrated in Figure 3.2. Total number of degrees of freedom in this equation system is about 700000. Computations have been performed on the same workstation and frequency domain analysis of the model takes about 1 minutes for one frequency.

By making frequency domain analysis of the shielded coil, we can observe the effect of the RF shield to the magnetic field homogeneity. For this purpose, we

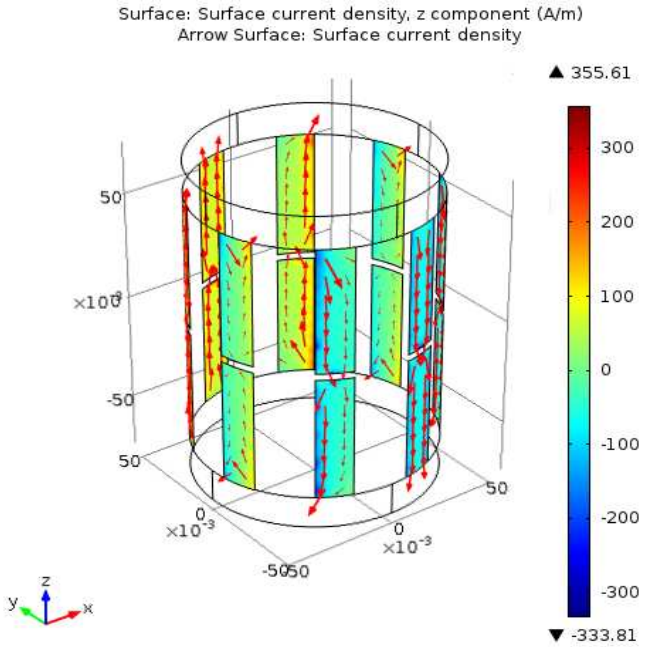

Figure 3.9: Illustration of the current distribution in the rungs with surface arrow plot

have driven the coil as quadrature excitation and compared the $|H^+|$ distributions for shielded and unshielded cases. For unshielded case, which we have already performed in the first simulation, magnitude images of H^+ at the central slice (z=0) and the corresponding line plot of $|H^+|$ along (x, y=0, z=0) line are shown in Figure 3.10.

For the shielded case, magnitude images of H^+ at the central slice (z=0) and the corresponding line plot of $|H^+|$ along (x, y=0, z=0) line are given in Figure 3.11.

As can be seen in Figure 3.11, uniformity of the H^+ increases when the RF shield, whose length is the same with the coil length and diameter is 1.4 times of the coil, is used. However, magnitude of the H^+ decreases with %13 because of the eddy currents induced in the shield and produce a magnetic field which is opposite to H^+.

Third simulation has been made for shielded and loaded 16-leg high-pass birdcage coil with a coil diameter of 24 *cm*, shield diameter of 28 *cm*, shield

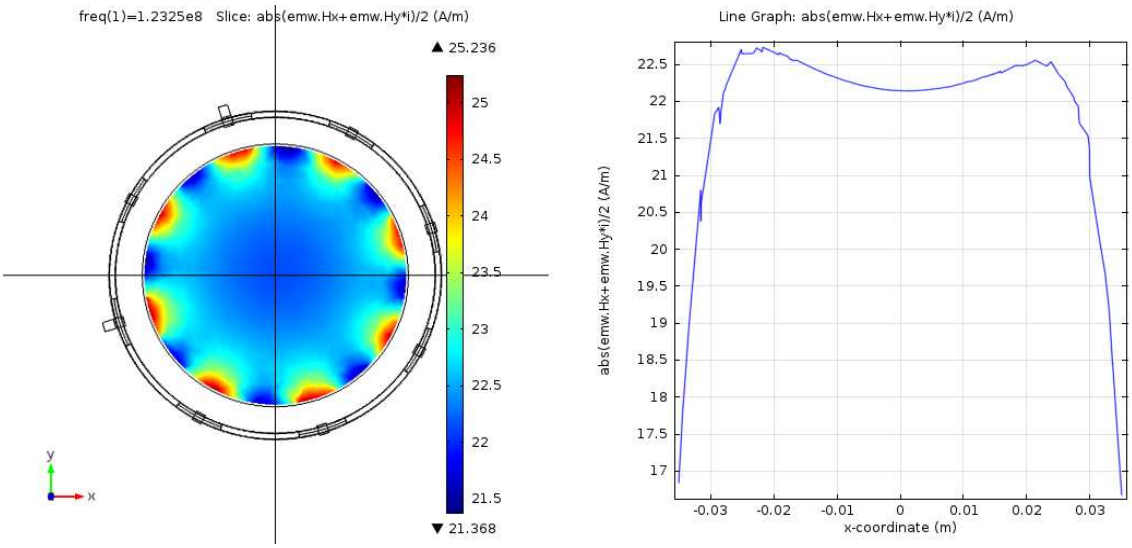

Figure 3.10: Magnitude image of H^+ at z=0 slice (left) and $|H^+|$ distribution along the (x, y=0, z=0) line (right) for unshielded low-pass birdcage coil

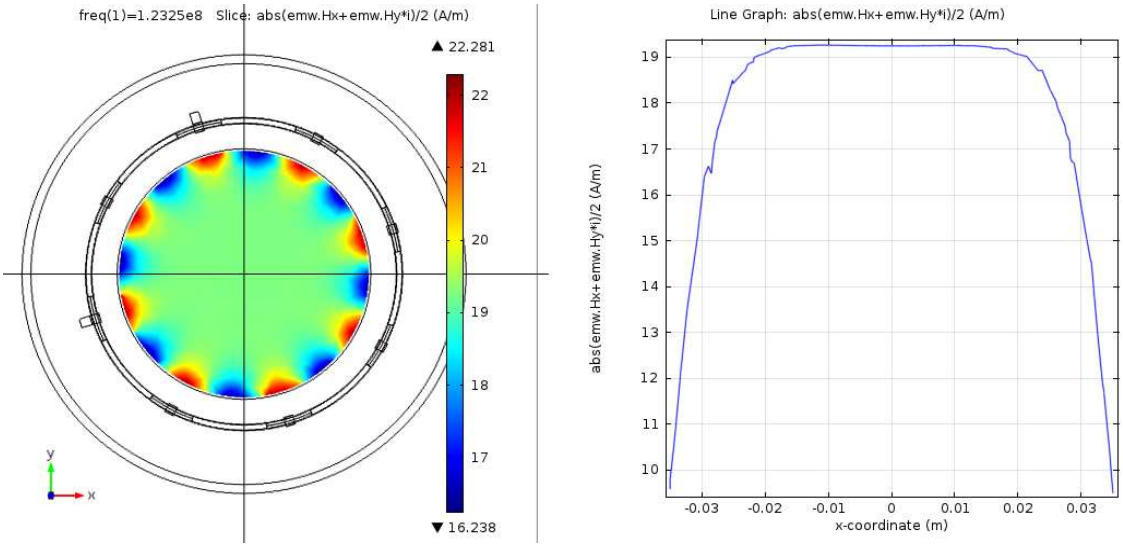

Figure 3.11: Magnitude image of H^+ at z=0 slice (left) and $|H^+|$ distribution along the (x, y=0, z=0) line (right) for shielded low-pass birdcage coil

length of 27 *cm*, rung length of 24 *cm*, and rung and end-ring width of 1.5 *cm*. Capacitance value is 49.4 pF and the simulation frequency is 123.2 *MHz*. We have put two cylindrical objects with different conductivity values and rectangular background inside the coil. Background conductivity is also different. Geometry of the model and the simulation phantom are shown in Figure 3.12.

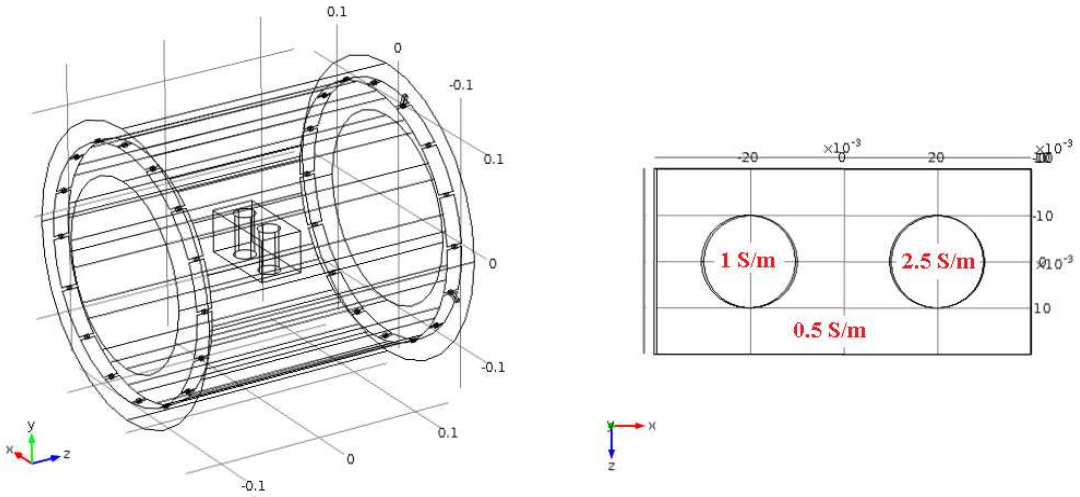

Figure 3.12: Geometric model of the shielded and loaded 16-leg high-pass birdcage coil (left) and simulation phantom with the conductivity values (right)

Total number of degrees of freedom in this equation system is about 2 million. Computations have been performed on the same workstation and frequency domain analysis of the model takes about 4 minutes for one frequency.

First, we can observe the magnitude images of the H^+ and H^- for the loaded birdcage coil and we can compare these results with the results of unloaded case in order to see the effects of the conductive objects to the magnetic field. Magnitude images of H^+ at z=0 slice for loaded and unloaded birdcage coils are given in Figure 3.13.

Figure 3.13 shows that conductive objects inside the coil slightly deteriorates the uniformity of the H^+. We are supposed to see this effect in also H^- images. For this purpose, magnitude images of H^- at z=0 slice for loaded and unloaded birdcage coils are illustrated in Figure 3.14.

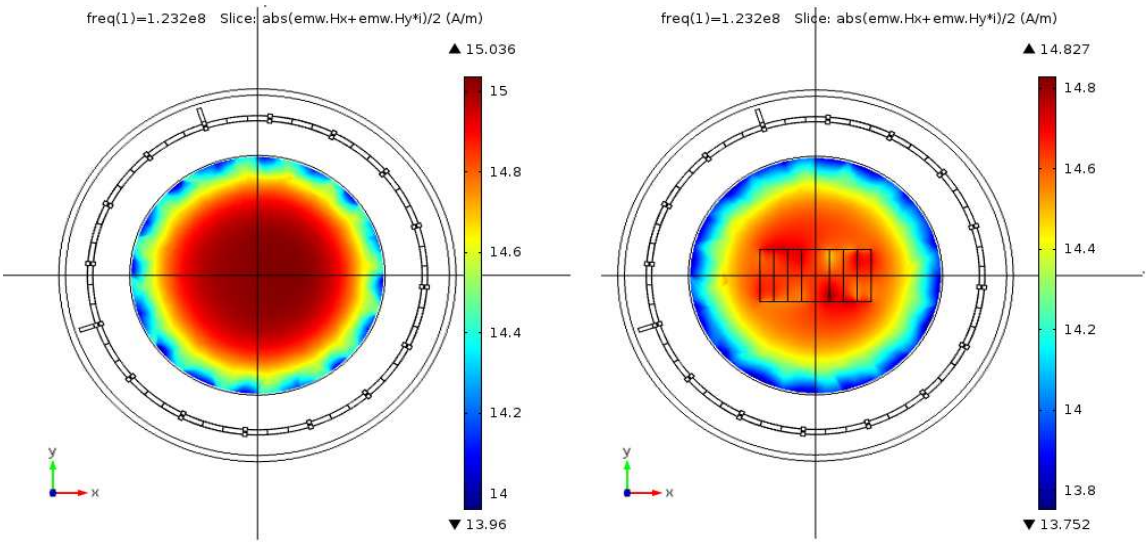

Figure 3.13: Magnitude images of H^+ for unloaded birdcage coil (left) and for loaded birdcage coil (right) at z=0

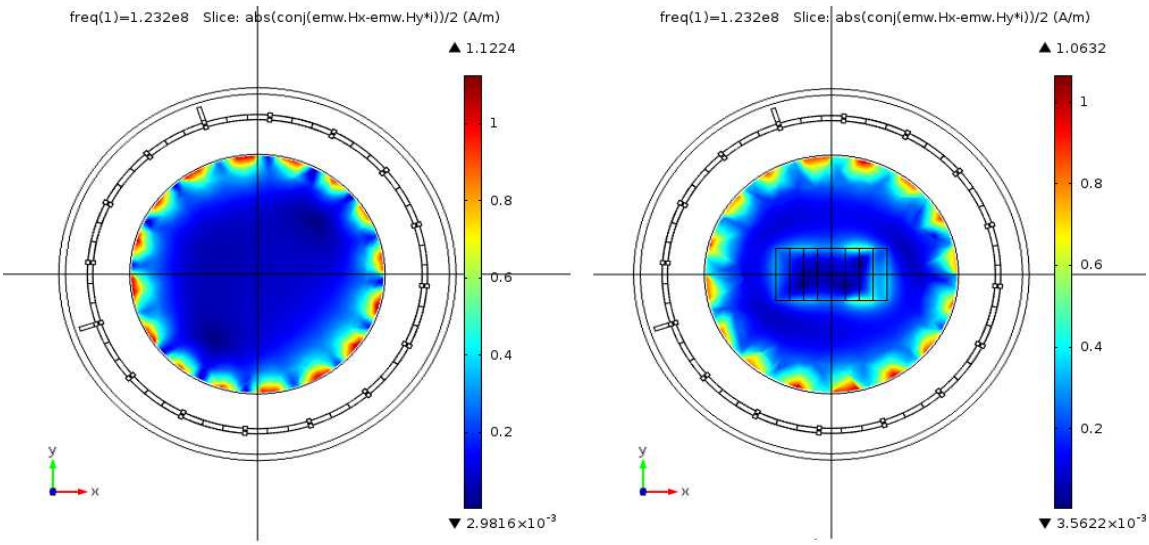

Figure 3.14: Magnitude images of H^- for unloaded birdcage coil (left) and for loaded birdcage coil (right) at z=0

By making frequency domain analysis of a loaded birdcage coil, we can also calculate the SAR distribution of the objects using the formula given as

$$SAR = \frac{\sigma |\mathbf{E}|^2}{\rho} \tag{3.6}$$

where σ and ρ are the conductivity and density of the object respectively. Normalized SAR distribution image at y=0 slice is shown in Figure 3.15.

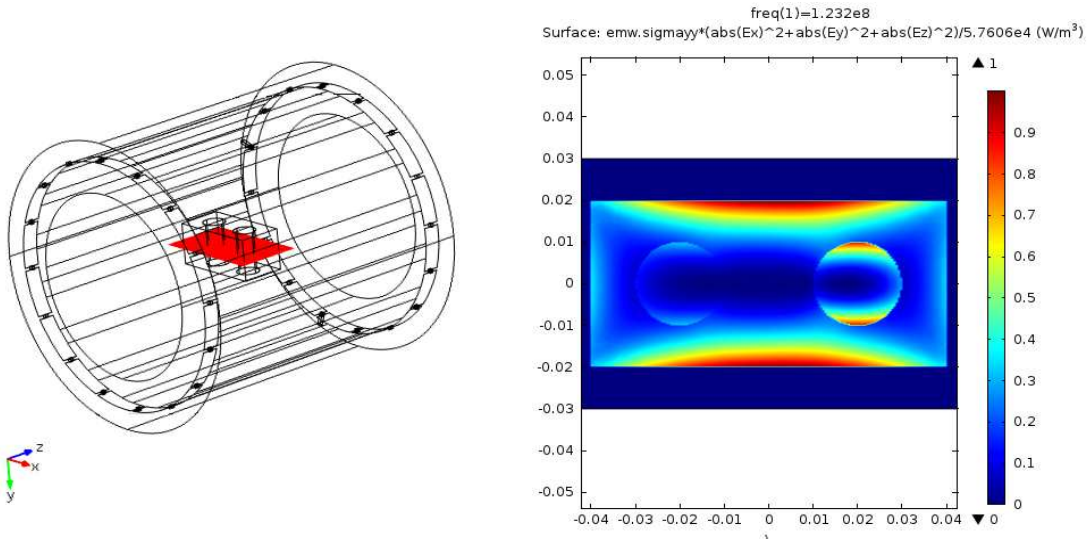

Figure 3.15: Normalized SAR distribution image (right) at the slice given on the left with a red color

In conclusion, one can make accurate simulations and observe the electromagnetic fields inside the coil by making frequency domain analysis of developed loaded (or unloaded) and shielded (or unshielded) birdcage coil models.

3.2.2 Capacitance Calculation of a Birdcage Coil using FEM based Optimization

In this section, a new method to calculate the necessary capacitance value for the birdcage coil in order to resonate the coil at the desired frequency is presented. This method is performed using an optimization with two different objective function in the frequency domain analysis of a one-port birdcage coil. One of them finds the capacitance value that maximizes the magnitude of the port impedance

($|Z_{11}|$) within the given capacitance range. We know that the magnitude of the port impedance reaches its maximum values at the resonant modes. By giving reasonable initial value, lower and upper bounds for the capacitance, optimum capacitance value which maximizes the $|Z_{11}|$ at the desired resonance frequency can be calculated. The other optimization process is to calculate the capacitance value that minimizes the variance of H^+ at the central region of the coil. We have already shown that magnetic field distribution inside the coil is uniform, especially in the central region of the coil, at the desired frequency. By using this information we can calculate the optimum capacitance value within a given capacitance range that minimizes the variance of H^+. These two optimization methods will be explained in detail in the following subsections.

3.2.2.1 Capacitance Calculation using $|Z_{11}|$ as an Objective Function

As previously mentioned, $|Z_{11}|$ of a birdcage coil takes its maximum values at the resonant modes. In order to observe this argument in a simulation environment, we have made frequency domain analyses of a 8-leg low-pass birdcage coil for the frequencies ranging from 115 MHz to 230 MHz with a step frequency of 1 MHz and for a given capacitance value. Simulation results for the $|Z_{11}|$ of this birdcage coil is illustrated in Figure 3.16.

As can be seen in Figure 3.16, for the constant capacitance value, there are four peaks of $|Z_{11}|$ corresponding to the four resonant modes (or frequencies) of the low-pass birdcage coil. As mentioned earlier, we are interested in the lowest frequency mode for the low-pass birdcage coils.

On the other hand, we can make this simulation by making the frequency constant and the capacitance value variable which is more appropriate for our situation since we want to find the capacitance for the known frequency. Simulation results of $|Z_{11}|$ for this condition is shown in Figure 3.17.

In Figure 3.17, for the constant frequency, there are four peaks of $|Z_{11}|$ same as in Figure 3.16. However, these do not correspond to the different resonant frequencies at this time since the frequency is constant and only the capacitance

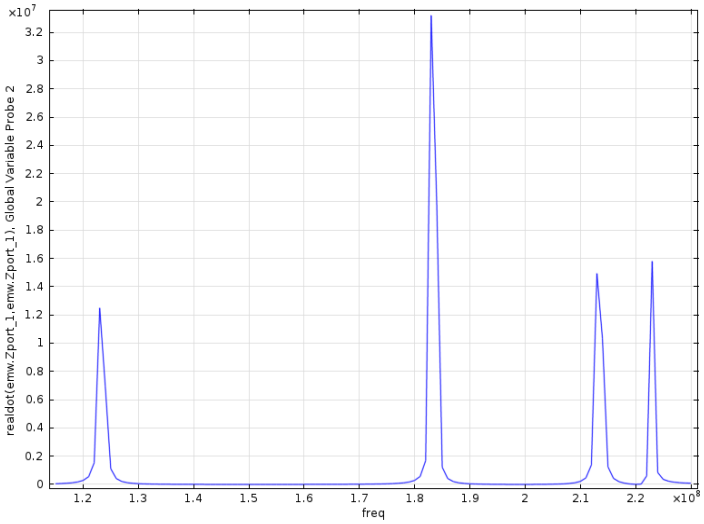

Figure 3.16: $|Z_{11}|$ of a 8-leg low-pass birdcage coil with respect to frequency (for the fixed capacitance)

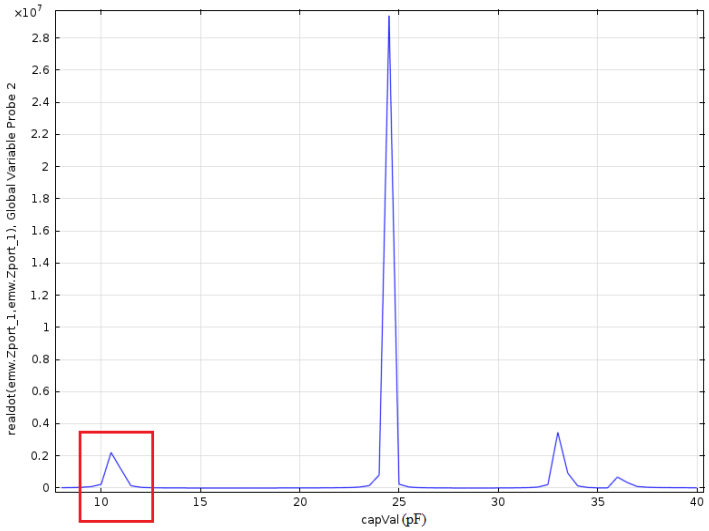

Figure 3.17: $|Z_{11}|$ of a 8-leg low-pass birdcage coil with respect to capacitance (for the constant frequency)

is changing. These are the different resonant modes that degenerates at the given constant frequency. For example, the peak value surrounded with the red box in Figure 3.17 implies that $m = 1$ mode at given frequency is obtained using a capacitance value about 10 pF. The other peak values implies that $m = 2$, $m = 3$, and $m = 4$ modes at given frequency are obtained using the capacitance values 24.5, 33, 36 pF respectively. From the view of optimization, $|Z_{11}|$ given in Figure 3.17 is the objective function (or cost function), capacitance value is the control variable and the task is to find the optimum capacitance value which maximizes the objective function $|Z_{11}|$ in a given capacitance range. For this purpose, we have used COMSOL Multiphysics optimization module.

COMSOL Multiphysics uses gradient-based optimization methods and these methods have some requirements such as that the objective function (or any constraint function) must be continuous and differentiable with respect to the control variable [15]. Furthermore, if there are more than one local maxima (or minima) in the objective function, gradient-based optimization method finds the one which is closest to initial value of the control variable. Therefore, we need to define a feasible set for the control variable in order to calculate the correct capacitance value, for example, red box given in Figure 3.17 can be the feasible set for our condition since we are interested in the lowest frequency mode.

For this purpose, we have first calculated a capacitance value using lumped circuit element model. This will be the our initial capacitance value. Before starting the optimization process, we need to define the lower and upper limits for the capacitance value. In other words, we need to define a feasible set for the optimization problem. In order to choose the capacitance range correctly, we have made frequency domain analysis of a birdcage coil at the desired frequency with twelve different capacitance whose values around the initial capacitance value. This analysis is made with a very coarse mesh and therefore it takes about 5 minutes. According to the results of this analysis, we have chosen a feasible set by looking at the graph of the objective function, $|Z_{11}|$. Then, we add new frequency domain analysis study with an optimization solver sequence instead of stationary solver used in previous section. In the optimization solver, there

are two algorithms: Sparse Non-linear OPTimizer (SNOPT) [19] and Levenberg-Marquardt algorithm [20] [21]. Among them, Levenberg-Marquardt algorithm can only be used when the objective function is in the least-square form, whereas SNOPT algorithm, which uses gradient-based optimization techniques, can be applied to any form of the objective function. Since our objective function, $|Z_{11}|$, is not in the least-square form, we have used SNOPT algorithm as an optimization solver method in the FEM model of birdcage coils. From the solver settings, we can set the optimization parameters such as optimality tolerance which determines the termination of the optimization process, maximum number of objective evaluations, objective contributions (if there are more than one object) and the gradient method. After adding study and the solver sequence we can start the optimization process using the FEM models of birdcage coil.

Note that, results for the calculated capacitance values using the proposed method are given under the *Experimental Results* chapter in order to compare the results of proposed method with the results of lumped circuit element model and the experimental results.

3.2.2.2 Capacitance Calculation using the Variance of H^+ as an Objective Function

As mentioned earlier, magnetic field distribution (H^+) inside the birdcage coil, especially at the central region of the coil, is uniform at the first resonant mode. Uniformity of the H^+ distribution deteriorates as the frequency moves away from the first resonant mode of the coil. In order to observe this argument in a simulation environment, we have first define a square plane region at the center of the birdcage FEM models which is shown in Figure 3.18.

Then, we have made frequency domain analysis at the desired frequency with different capacitance values and calculated the variance of H^+ at this square shaped boundary for each capacitance value using the formula given as

$$Var(H^+) = \frac{1}{S_\Omega} \int_\Omega |H^+ - \mu|^2 d\Omega \tag{3.7}$$

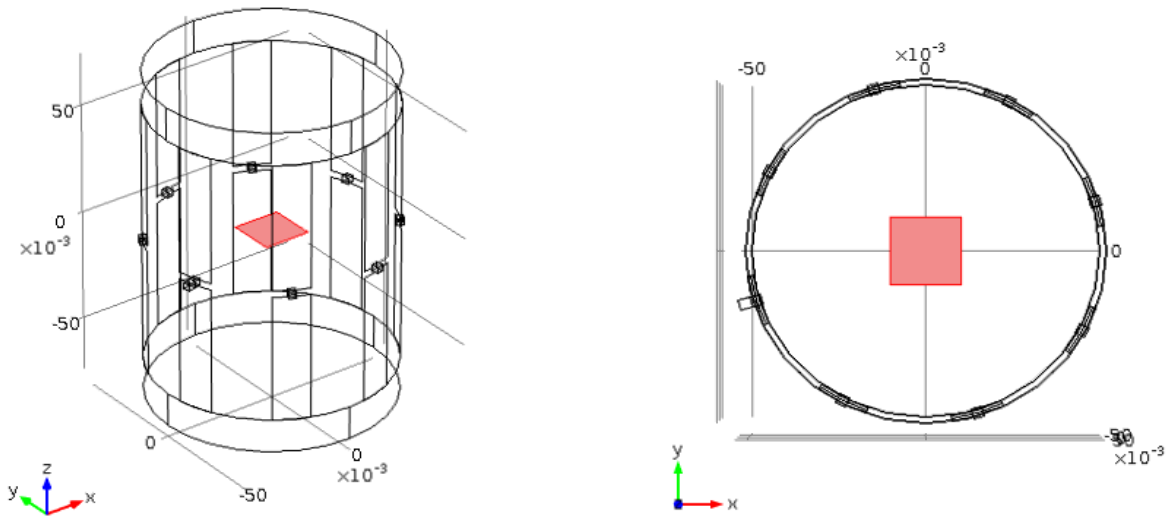

Figure 3.18: Geometric model of a 8-leg low-pass birdcage coil with a square shaped boundary at the center of the coil

where Ω is the surface boundary, S_Ω is the area of the boundary, and μ is the mean (or average) of H^+ at this boundary.

Simulation results for the variance of H^+ at this square boundary is illustrated in Figure 3.19.

As can be seen in Figure 3.19, variance of H^+ has only one minimum point for the given capacitance range. From the view of optimization, we can think that the variance of H^+ is our objective function and the capacitance value is the control variable. The task is to find the optimum capacitance value which minimizes the variance of H^+ at the boundary which is placed at the center of the coil.

For this purpose, we have made the same steps as we did in the previous section for the optimization process. The only difference is to use the variance of H^+ as an objective function instead of using $|Z_{11}|$. Results for the calculated capacitance values using the proposed method are given under the *Experimental Results* chapter.

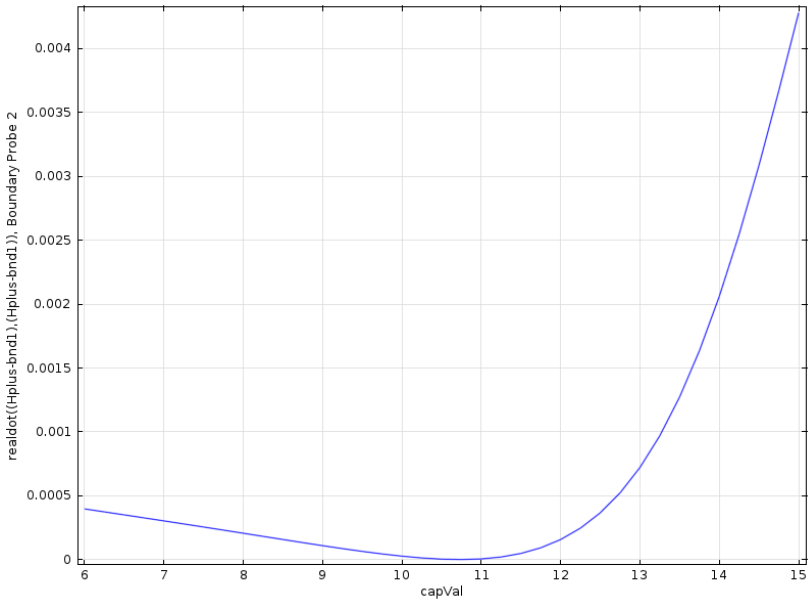

Figure 3.19: Variance of H^+ at the square plate with respect to capacitance

3.2.3 Eigenfrequency Analysis of a Birdcage Coil

In this section, eigenfrequency analysis of a birdcage coil, which is used to determine the resonant modes of the birdcage coil, is presented. Same as the previous methods, we use developed FEM models of low-pass and high-pass birdcage coil in this analysis. Model geometry is a bit different than the model geometry constructed in the frequency domain analysis. In eigenfrequency analysis, no sources are applied and therefore we do not use the lumped port boundary condition for this analysis. Geometric model of the low-pass and high-pass birdcage coil used in eigenfrequency analysis are shown in Figure 3.20.

As can be seen in Figure 3.20, no lumped port boundary is used to apply voltage. There are only parallel plate capacitors placed on the rungs or end rings.

Electromagnetic wave equation used in the time harmonic and eigenfrequency problems was given in Equation 3.2. In the case of eigenfrequency analysis ω is the unknown variable in Equation 3.2 and the eigenvalue, λ, can be expressed in

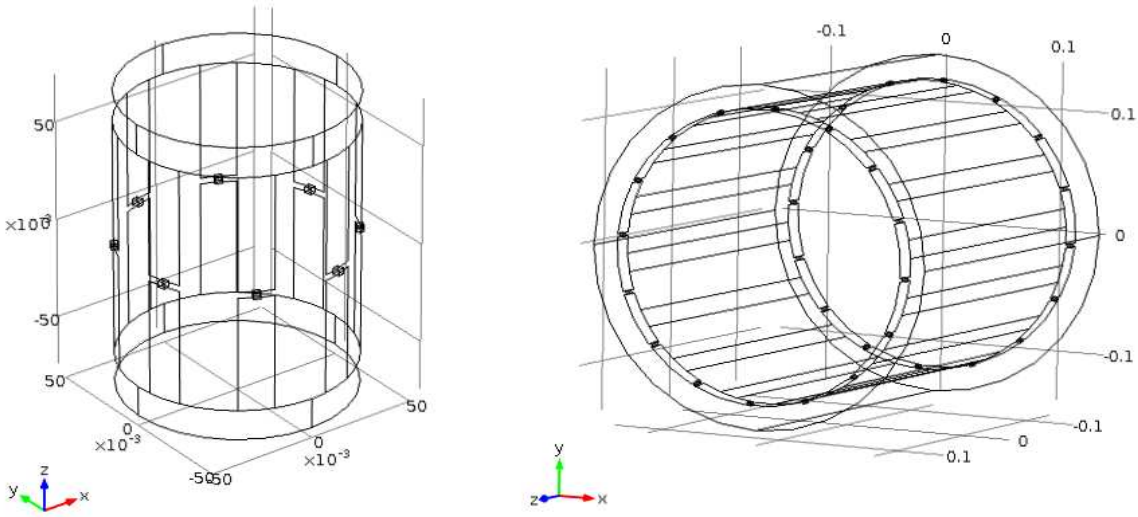

Figure 3.20: Geometric model of unshielded 8-leg low-pass birdcage coil (left) and shielded 16-leg high-pass birdcage coil (right) used in eigenfrequency analysis

terms of ω as

$$-\lambda = -\delta + j\omega \tag{3.8}$$

where imaginary part of the eigenvalue, ω, corresponds to the eigenfrequency and the real part, δ, represents the damping factor. Eigenvalue can be complex valued as given in Equation 3.8 when the model includes some lossy parts such as conductive objects, when boundaries are modeled as scattering boundary condition, or when domains are modeled as perfectly matched layers. In a such condition, we can express the quality factor (Q) in terms of eigenfrequency and damping factor as

$$Q = \frac{\omega}{2|\delta|} \tag{3.9}$$

It is important to note that we can calculate the Q-factor of the birdcage coil using the Equation 3.9.

After modeling the coil geometry, adding physics and boundary conditions, and generating mesh as explained in the first section of this chapter, we need to add necessary study and the solver sequence for eigenfrequency analysis in COMSOL Multiphysics. This step is explained under the following subsection.

3.2.3.1 Study and Solver Sequence

For eigenfrequency analysis, we first add *Eigenfrequency Study* as the study node. From the study settings, we can define the number of eigenfrequencies which the solver finds and the frequency point around which the solver looks for the eigenfrequencies. Then, we add *Eigenvalue Solver* as the solver sequence to solve the FEM based generalized eigenvalue system which is given as [15]

$$(\lambda - \lambda_0)^2 EU - (\lambda - \lambda_0)DU + KU + N_F\Lambda = 0 \tag{3.10}$$

$$NU = 0 \tag{3.11}$$

where λ is the eigenvalue, λ_0 is the linearization point, E is the mass matrix, U is the solution vector, D is the damping matrix, K is the stiffness matrix, N_F is the constraint force Jacobian matrix, Λ is the Lagrange multiplier vector, and N is the constraint Jacobian matrix. If the mass matrix (E) in Equation 3.10 is 0, eigenvalue problem will be linear. If E is non-zero, eigenvalue problem will be quadratic which needs a special treatment to transform the problem into a linear eigenvalue problem.

Eigenvalue solver starts the computation of the eigenfrequencies by linearizing the problem around the linearization point, whose default value is 0. In non-linear eigenfrequency problems, using this default value of the linearization point causes an error because the λ is generally in the denominator in the equation system and leads to division by zero. In our situation, using scattering boundary condition leads to this problem and therefore we need to specify a linearization point (λ_0) in order to avoid this problem. Instead of specifying the linearization point manually, we can use the solution of any study as the linearization point of the eigenfrequency study.

After making the necessary adjustments for the study and solver sequence, we can compute the eigenfrequencies of the model which correspond to the resonant modes of the birdcage coil. We can also observe the electromagnetic field or variable distributions at these resonant modes. Simulation results are given in the following section.

3.2.3.2 Simulation Results

First simulation has been made for unshielded and empty 8-leg low-pass birdcage coil with a diameter of 10 *cm*, rung length of 11.5 *cm*, and rung and end-ring width of 1.5 *cm*. Capacitance value used on the rungs is 10.3 *pF*. Number of eigenfrequencies is specified as 8 and the linearization point is given as $(-j2\pi 120 \times 10^6)$. Total number of degrees of freedom in the equation system is about 600000. Computations have been performed on the same workstation and eigenfrequency analysis of the model takes about 10 minutes.

There are four distinct resonant modes calculated in this eigenfrequency analysis. Results for the magnitude images of H^+ inside the coil at these four resonant modes are given in Figure 3.21.

As can be seen in Figure 3.21, calculated eigenfrequencies are complex valued in which the real part corresponds to under-damped natural resonance frequency, f_0, and the imaginary part represents the damping factor, δ. We can find the damped natural resonance frequency, f_d, using the equation given as

$$f_d = f_0\sqrt{1-\zeta^2} \tag{3.12}$$

where ζ is the damping ratio and defined as

$$\zeta = \frac{\delta}{2\pi f_0} \tag{3.13}$$

Since $\delta << f_0$ for the calculated eigenfrequencies given in Figure 3.21, we can write the damped natural frequency as $f_d \approx f_0$. Therefore we can say that first resonant mode of the coil, which is the desired mode ($m = 1$), is found at 123.27 *MHz*, and the other modes, $m = 2$, 3, and 4, are found at 182.57 *MHz*, 211.83 *MHz*, and 220.84 *MHz* respectively.

As mentioned earlier, we have found four distinct resonant modes for 8-leg low-pass birdcage coil. Among these modes, $m = 1$, 2, and 3 are the degenerate mode pairs and $m = 4$ is the singlet mode. We know that, degenerate mode pairs are actually two modes that have the same resonance frequency but represented

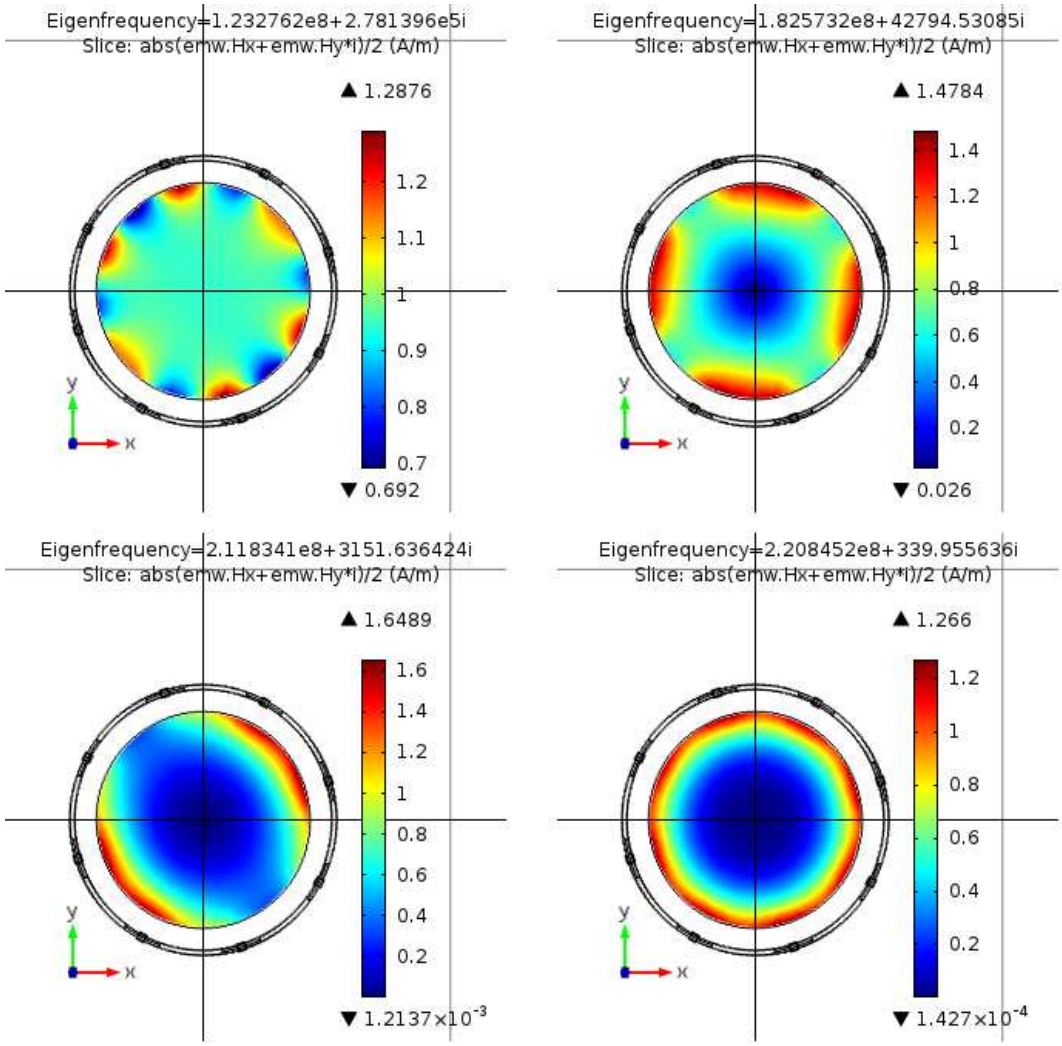

Figure 3.21: Magnitude images of H^+ at the resonant modes of the coil. (m=1 (left-top), m=2 (right-top), m=3 (left-bottom), and m=4 (right-bottom))

with the single m and these two modes produces magnetic fields which are perpendicular to each other. We can also observe these two magnetic fields in this analysis. For $m = 1$ mode, magnitude images of H^+ at these two resonant modes are given with the surface arrow plots in Figure 3.22.

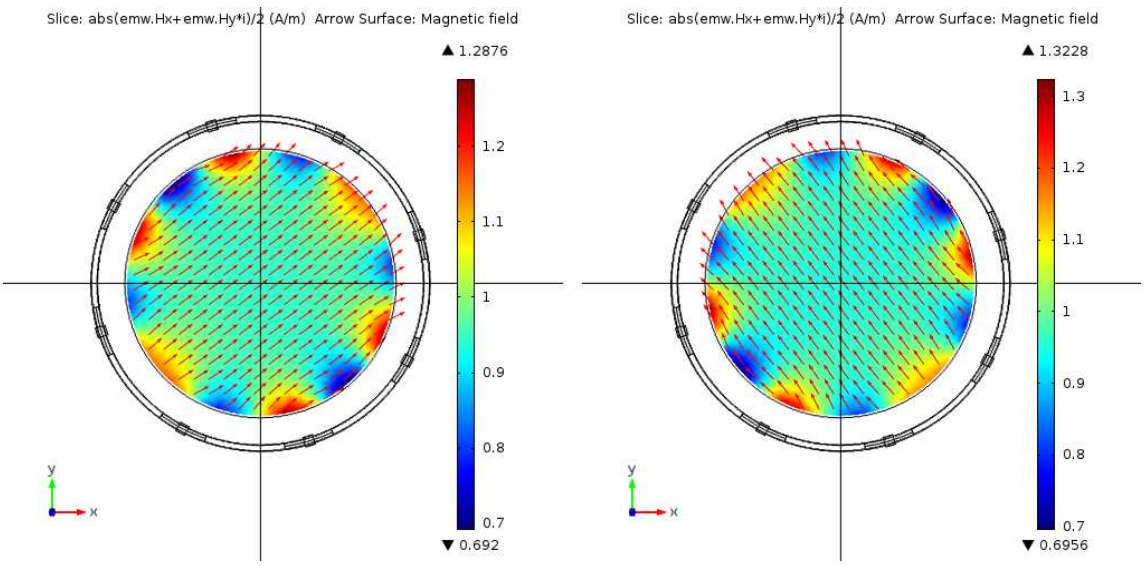

Figure 3.22: Magnitude images of H^+ for the frequencies found at 123.276 MHz (left) and 123.299 MHz (right) of $m = 1$ mode

Second simulation has been made for shielded and empty 16-leg high-pass birdcage coil with a coil diameter of 24 *cm*, shield diameter of 28 *cm*, shield length of 27 *cm*, rung length of 24 *cm*, and rung and end-ring width of 1.5 *cm*. Capacitance value is 49.4 *pF*. Number of eigenfrequencies is specified as 16 and the linearization point is given as $(-j2\pi 120 \times 10^6)$. Total number of degrees of freedom in this equation system is about 2 million. Computation has been performed on the same workstation and have taken about 35 minutes.

There are eight distinct resonant modes calculated in this eigenfrequency analysis. Instead of observing these modes as we did in the previous simulation, we want to investigate another mode, which is previously mentioned as co-rotating/anti-rotating or end ring resonant mode, $m = 0$. In this mode, currents flow only in the end rings so that no transverse electromagnetic field is produced inside the coil. Eigenfrequency analysis can also calculate this mode and we can observe the field distribution at the transverse plane and current

distribution in the rungs and end rings. Magnitude images of H^+ at the central slice (z=0) and the arrow plot of surface current density in rungs and end rings at two frequencies of $m = 0$ mode are illustrated in Figure 3.23.

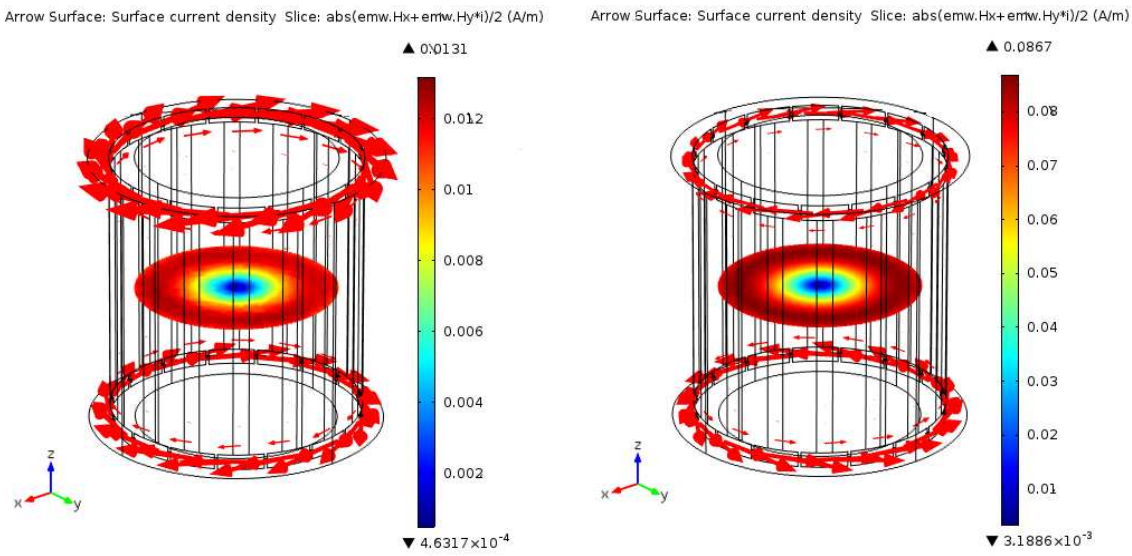

Figure 3.23: Magnitude images of H^+ and the arrow plot of surface current densities for the frequencies found at 150.518 MHz (left) and 150.581 MHz (right) of $m = 0$ mode

As can be seen in Figure 3.23, $m = 0$ has two modes as the other degenerate mode pairs. One of these modes corresponds to the co-rotating mode in which the currents in the end rings are rotating in the same direction and the other mode corresponds to the anti-rotating mode in which the currents in the end rings are in the opposite direction. Since no current flows in the rungs, transverse magnetic field inside the coil shown in Figure 3.23 is significantly small.

In conclusion, one can calculate the resonant modes of the birdcage coil and observe any electromagnetic fields and variables at these resonant modes. Simulation results of the eigenfrequency analysis will be compared with the experimental results and the results of the lumped circuit element model under the *Experimental Results* chapter.

3.3 Discussion and Conclusion

In this chapter, we have presented the development of low-pass and high-pass birdcage coil FEM models and three simulation methods which are performed using these models in COMSOL Multiphysics.

First method is the frequency domain analysis which is used to simulate practical birdcage coils used in MRI for a given frequency and the capacitance value. By performing this analysis, one can calculate the electromagnetic fields inside the birdcage coil for any scenario and produce simulated B_1 data which is widely used in the MR based electromagnetic tissue property mapping algorithms such as MREPT. Furthermore, this analysis can be used to simulate loaded birdcage coils at higher frequencies in order to investigate the SAR at any object at these frequencies. Additionally, one can investigate how geometric changes in the coil elements or the objects that have different material properties inside the coil affects the field solutions of the birdcage coil. Since the field strength of MRI Scanner in Ulusal Manyetik Rezonans Aratrma Merkezi (UMRAM) that we use for our MR experiments is about 2.893 T, simulation results are given at 123.2 MHz for practice. The important point here is to find the necessary capacitance value which makes the coil resonate at 123.2 MHz. This is accomplished by using the second method we have proposed.

Second method is the capacitance calculation of a birdcage coil using FEM based optimization. In this method, optimum capacitance value at given resonance frequency is calculated using an optimization with two different objective functions: $|Z_{11}|$ and the variance of H^+. By looking at these two objective functions given in Figure 3.17 and Figure 3.19 respectively, we can see that $|Z_{11}|$ in Figure 3.17 forms sharp peaks, whereas the variance of H^+ in Figure 3.19 forms a shallow minimum. Since we want to find the capacitance value which maximizes (or minimizes) the objective function, using $|Z_{11}|$ as an objective function will give more reliable results because the numerical errors in the computation is more dominant at the shallow regions and this may lead to misdetection of the minimum value of the variance of H^+. On the other hand, using only $|Z_{11}|$ as an objective function may also give wrong results if the objective function

includes more than one maximum point in the given set. Therefore, we can use the variance of H^+ to determine the feasible set since it has only one minimum point. Then, we can make the optimization using $|Z_{11}|$ as an objective function with this determined set. We believe that this approach will help to eliminate any possible errors in the optimization process.

Third method is the eigenfrequency analysis which is used to calculate not only the resonant modes of the birdcage coil but also the electromagnetic fields or variables distributions at these resonant modes. This analysis provides information about the resonance behavior of the coil and therefore tuning and matching procedure of the working mode ($m = 1$) can be safely done without interfering with the other modes. Further more, we can also determine the quality factor of the birdcage coil loaded with a conductive object by making eigenfrequency analysis.

Before comparing the results of these three methods with the experimental results and lumped element model results, we need to be sure that they are first consistent with each other. For this purpose, we have made some trials. For example, we have used the capacitance value, which is calculated using FEM based optimization at given frequency, in the eigenfrequency analysis and compared the first resonant frequency calculated in eigenfrequency analysis with the frequency given in FEM based optimization. We have also made a frequency domain analysis for the capacitance, which is calculated by using FEM based optimization method, and checked if the H^+ is uniform or not for this capacitance value in the frequency domain analysis. In the end, we are sure that they are perfectly consistent with each other.

In order to provide convenience for the coil designers and the researchers in the field of MRI to make these three simulation methods easily and according to the parameters they specify, we have developed two user-friendly software tools using MATLAB GUI which connect to the COMSOL Multiphysics server and make all the FEM based design and simulations in the background. These software tools will be explained in the next chapter.

Chapter 4

SOFTWARE TOOLS FOR DESIGNING AND SIMULATING A BIRDCAGE COIL

In this chapter, two different software tools, that we have developed to make the FEM based simulation methods explained in the previous chapter according to the user-specified parameters easily, are presented. One of the software tools is used to calculate the capacitance value of a birdcage coil using the FEM based optimization method and the other one is used to make frequency domain and eigenfrequency analysis of a birdcage coil. Both of the software tools have been developed in MATLAB and have user-friendly graphical user interface (GUI). User can make any of the three simulation methods for any type of birdcage coil by only specifying the coil type, dimensions and necessary parameters from the GUI of the program. Then, software tools make all the design and simulation steps such as modeling the coil geometry, adding physics and boundary conditions, generating mesh and computing the solutions by connecting the COMSOL Multiphysics server in the background. When the simulation is finished, the user can import the model from the server and observe the any electromagnetic fields

and variables in the solution domain. In the following two sections, these software tools will be explained in detail.

4.1 A Software Tool for Frequency Domain and Eigenfrequency Analysis of a Birdcage Coil

First software tool is used to make two electromagnetic analyses of a birdcage coil: frequency domain and eigenfrequency analyses. GUI of the program is given in Figure 4.1.

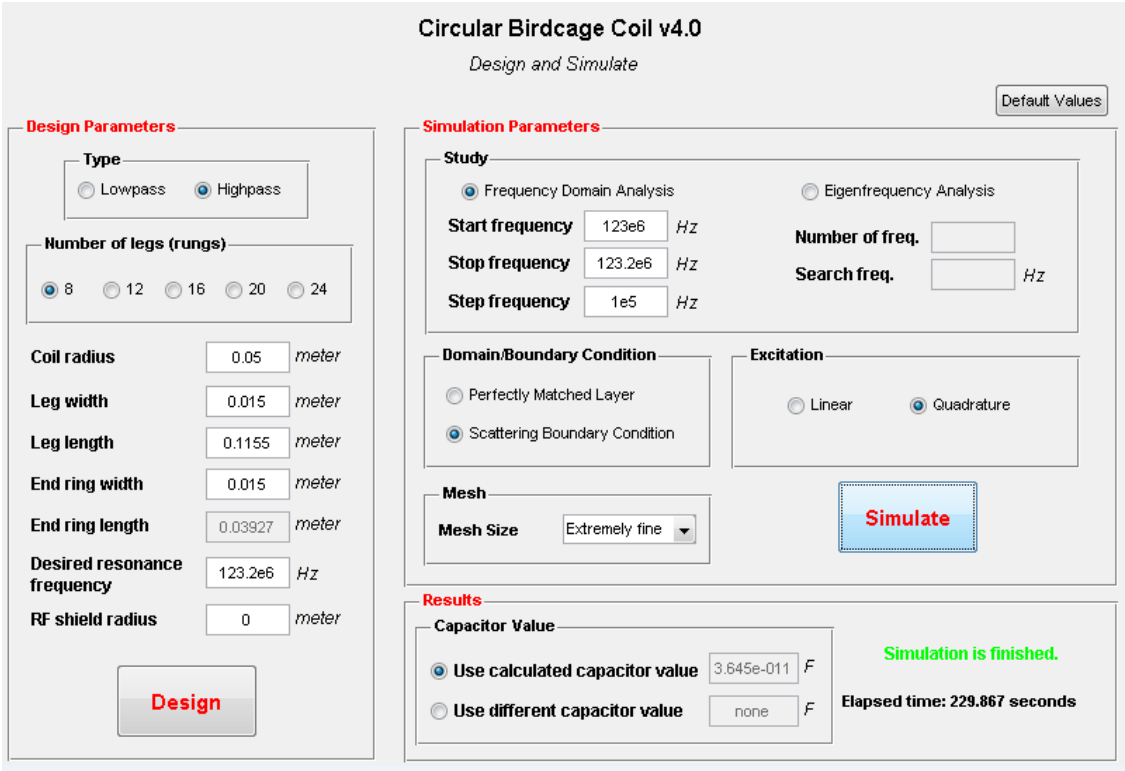

Figure 4.1: Graphical User Interface (GUI) of the software tool used in frequency domain and eigenfrequency analyses

As can be seen in Figure 4.1, there are three sections of this software tool: Design parameters, simulation parameters and results.

The user first starts with specifying the design parameters that are coil type,

number of legs and coil dimensions. For the unshielded birdcage coil simulations, RF shield radius must be specified as zero. Then, by clicking the *Design* button, the tool calculates the necessary capacitance value using lumped circuit element model and calculated capacitance value appears in the results section of the program.

Second, simulation parameters should be specified. For this purpose, the user starts with selecting the study type and specifying the parameters that correspond to selected study. If frequency domain analysis is chosen, for example, frequency range for this analysis must be specified. In order to make a frequency domain analysis at a single frequency, start and stop frequency should be the same and equal to the frequency at which the simulation is made and the frequency step can be any value other than zero. Then, the user chooses one of the boundary conditions for the solution domain to prevent reflections from the outer boundary and selects the excitation type in order to produce linearly or circularly polarized field inside the birdcage coil. If eigenfrequency analysis is chosen, on the other hand, the user should specify the number of eigenfrequencies, which the solver finds, and the frequency point around which the solver looks for the eigenfrequencies. Since no source is applied in eigenfrequency analysis, excitation part is disabled. For both analysis, desired mesh size is selected from the mesh selection part. Before the simulation starts, the user can specify different value for the capacitance whose default value is calculated using lumped circuit element model. After all the necessary parameters are specified, the user can start the simulation by clicking the *Simulate* button.

When the simulation is started, the program connects to the COMSOL Multiphysics server via COMSOL Multiphysics Livelink for MATLAB environment and makes the FEM based design and simulations according to the user-specified parameters. During the simulation, the tool informs the user about which step is being performed at that moment by displaying the step in the results section. When the simulation is finished, the program notifies the user and simulation results can be observed in COMSOL Multiphysics by importing the computed model from the server. It is important to note that simulation results can also be

observed in MATLAB environment but displaying the results in COMSOL Multiphysics is easier and also offers to make changes in the model. For example, after making frequency domain analysis of 16-leg high-pass birdcage coil by using this software tool, we can import the computed model to the COMSOL Multiphysics environment, put any arbitrary object inside coil and make the simulation for loaded birdcage coil easily.

4.2 A Software Tool for Capacitance Calculation of a Birdcage Coil

The other software tool is used to calculate the necessary capacitance value of a birdcage coil in order to resonate the coil at the specified frequency. GUI of the program is illustrated in Figure 4.2

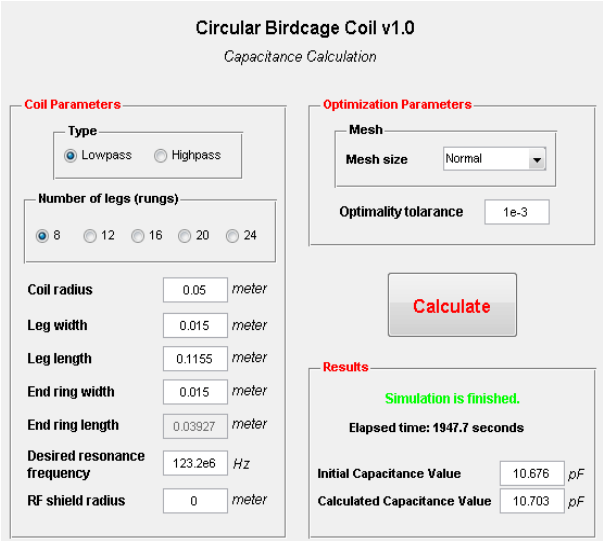

Figure 4.2: Graphical User Interface (GUI) of the software tool used in capacitance calculation

As given in Figure 4.2, this software tool has three sections. One of the sections, in which the user specify the coil parameters, are the same with the previous one. After specifying the coil parameters, the user chooses the mesh size and define the optimality tolerance from the optimization parameters section.

As previously mentioned, optimality tolerance determines when the optimization process terminates. After specifying all necessary parameters, optimum capacitance value can be calculated by clicking the *Calculate* button.

When the simulation starts, the program first calculates a capacitance value using lumped circuit element model. This capacitance value is used to define a capacitance range for the next step which is the frequency domain analysis of a birdcage coil with a very coarse mesh for twelve different capacitance values. This is called parametric sweep study in which the capacitance value is the variable parameter. At the end of this study, the program displays two objective functions, $|Z_{11}|$ and $Var(H^+)$, with respect to capacitance and asks the user which objective function will be used for the optimization process. As an example, parametric study results for the birdcage coil, whose properties and dimensions are given as in Figure 4.2, is illustrated in Figure 4.3.

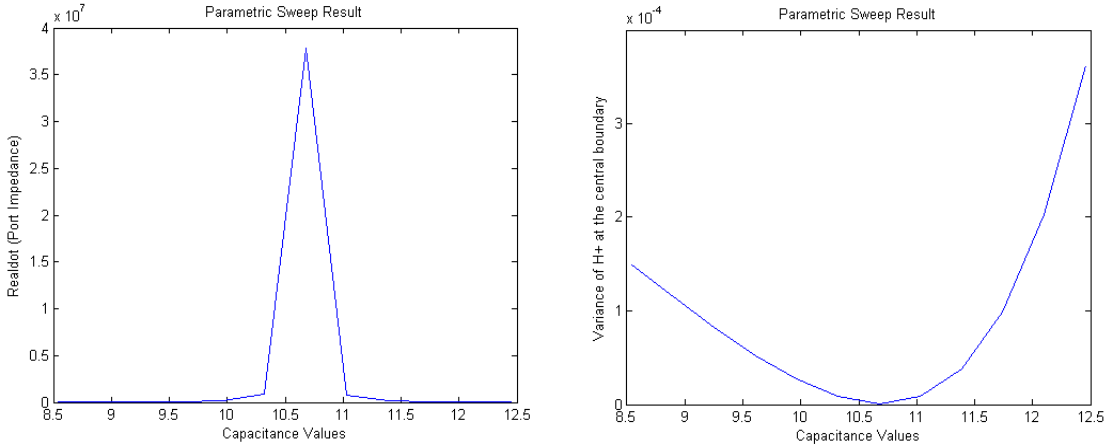

Figure 4.3: Parametric study results of the objective functions: $|Z_{11}|$ (left), variance of H^+ (right)

When the user chooses one of the objective functions, the program wants from the user to specify the initial value, lower and upper bounds for the capacitance to be used in the optimization process. This selection is performed by clicking the three points, which are corresponding to lower bound, initial value and upper bound respectively, on the selected objective function figure. This selection is illustrated in Figure 4.4 for the objective function, $|Z_{11}|$.

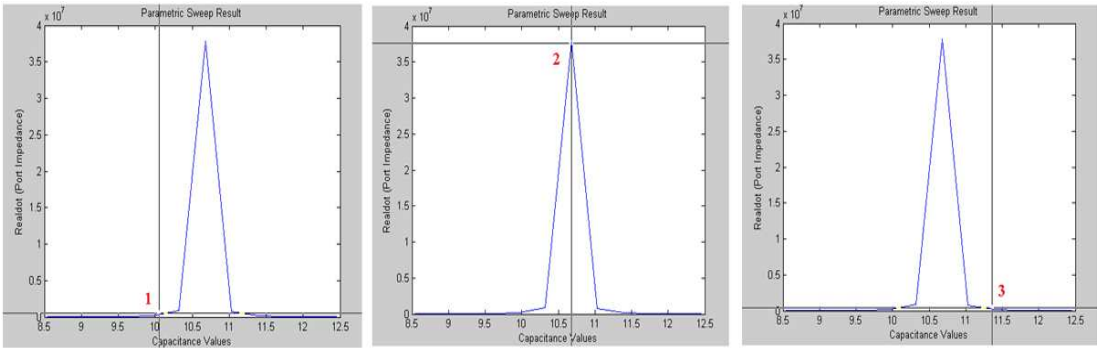

Figure 4.4: Illustration of the selection of the lower bound (left), initial value (middle), and upper bound (right) for the capacitance value

After specifying the capacitance ranges, program starts to optimization process with the specified mesh size. When the simulation is finished, initial value given for the capacitance and the calculated capacitance are shown in the results section, which can be seen in Figure 4.2.

4.3 Discussion and Conclusion

In this chapter, we have presented two software tools that are used to make design and simulation calculations of a low-pass and high-pass birdcage coil easily. We believe that these software tools provide many conveniences to the users. For example, modeling a birdcage coil in a 3D simulation environment is a difficult task because of the complex geometry of the birdcage coil. By using these software tools, any birdcage coil is modeled geometrically, necessary boundary conditions are assigned to the coil elements, mesh and study properties are set automatically. As a result, the user can perform any of the simulation methods discussed in Chapter 3 properly.

The program codes are written in MATLAB and COMSOL Multiphysics Livelink for MATLAB environment is used. Using this environment provides us to perform any COMSOL actions in MATLAB. When the simulations are finished, computed models can be imported from the server to the COMSOL Multiphysics and any electromagnetic field and variable distribution can be observed.

Chapter 5

EXPERIMENTAL RESULTS AND COMPARISON WITH NUMERICAL ANALYSES

In this chapter, experimental results for the resonant modes and capacitance values of two handmade birdcage coils are presented. These coils are low-pass and high-pass birdcage coils and they are illustrated in Figure 5.1 without capacitors.

As can be seen in Figure 5.1, they are both 8-leg birdcage coils with a diameter of 10 cm and are built on plexiglass tubes with a length of 16.5 cm. The width of the copper strips used to construct rungs and end-rings is 1.5 cm. Rung length of the low-pass birdcage coil is about 11.55 cm, whereas rung length of the high-pass birdcage coil is about 11.25 cm. They are both constructed as one-port and unshielded birdcage coil.

Experimental results can be discussed under two sections. One of them is the results of the resonant modes of the birdcage coils. For this purpose, we have made measurements for five different capacitance values (Dielectric Laboratories High-Q Multi-Layer and Broadband Blocking Capacitors) for each birdcage coil and measured the S_{11} of the coils using Agilent Technologies E5061A (300 kHz - 1.5 GHz) Network Analyzer in order to obtain the resonant modes of the coil.

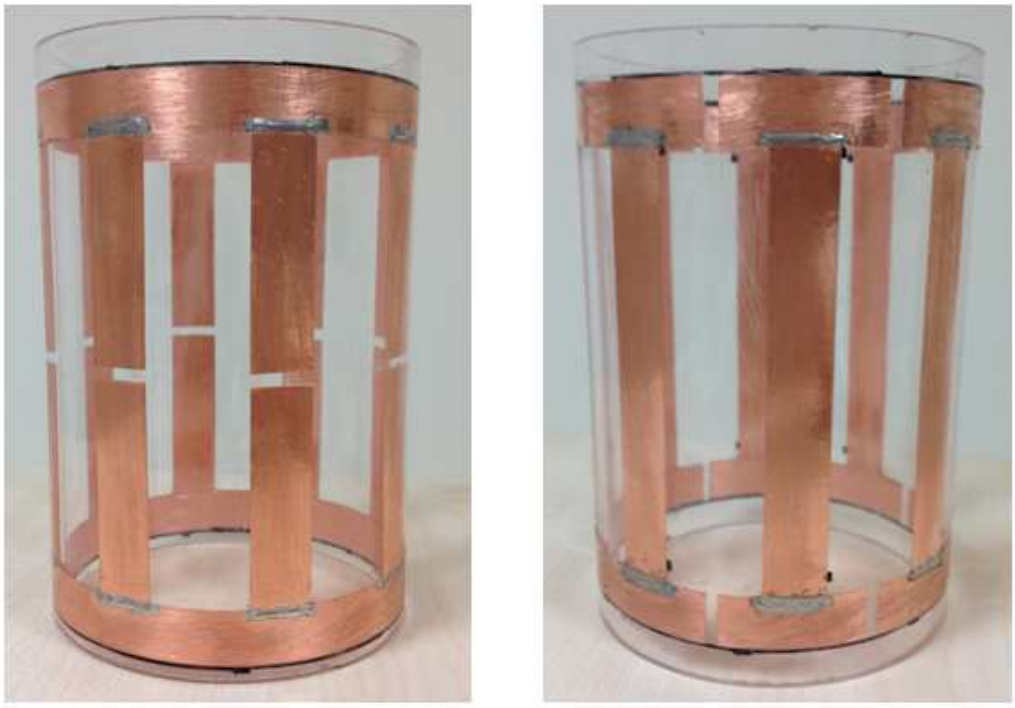

Figure 5.1: Constructed two handmade birdcage coils. Low-pass type (left) and high-pass type (right)

Then, these experimental results are compared with the results of the software tool called MRIEM presented in [9] and the results of FEM based eigenfrequency analysis tool (FEM-EFAT) we have proposed. The other section is the comparison of the capacitance values used in the experiments with the capacitance values calculated using the software tool called BirdcageBuilder presented in [5] and FEM based optimization tool (FEM-OPT) we have proposed.

5.1 Measured and Calculated Resonant Modes

In this section, experimental results for the resonant modes of the unshielded 8-leg low-pass and high-pass birdcage coils, which are shown in Figure 5.1, are presented for five different capacitance values. Then, these experimental results are compared with the results of MRIEM (a software tool that uses the lumped circuit element model presented in [9], and can be downloaded from the link

http://jin.ece.illinois.edu/mriem.dir/mriem.html) and the results of FEM-EFAT we have developed.

5.1.1 Results of the High-pass Birdcage Coil

In order to compare the measured and calculated results of the resonant modes of 8-leg high-pass birdcage coil, the results for each capacitance value are given in a separate table. For the capacitance value of 100 pF ($\pm\%2$), 30 pF ($\pm\%2$), 15 pF ($\pm\%2$), 7.5 pF ($\pm 0.25pF$), and 3.3 pF ($\pm 0.25pF$), measured and calculated resonant modes are given in Tables 5.1 to 5.5 respectively.

Modes	Experimental Results (MHz)	MRIEM (MHz)	FEM-EFAT (MHz)
m=4	52.13	51.91	52.67
m=3	53.63	54.24	54.58
m=2	59.63	62.82	61.11
m=1	75.25	86.14	75.36
m=0	107.6	-	108.3

Table 5.1: Measured and calculated resonant modes of 8-leg high-pass birdcage coil for the capacitance of 100 pF

Modes	Experimental Results (MHz)	MRIEM (MHz)	FEM-EFAT (MHz)
m=4	94.43	94.76	95.58
m=3	97.33	99.03	99.02
m=2	106.0	114.68	110.74
m=1	131.4	157.27	136.18
m=0	195.2	-	196.06

Table 5.2: Measured and calculated resonant modes of 8-leg high-pass birdcage coil for the capacitance of 30 pF

Modes	Experimental Results (MHz)	MRIEM (MHz)	FEM-EFAT (MHz)
m=4	131.2	134.02	134.1
m=3	134.0	140.05	138.87
m=2	143.8	162.19	155.08
m=1	182.5	222.41	189.92
m=0	264.2	-	275.1

Table 5.3: Measured and calculated resonant modes of 8-leg high-pass birdcage coil for the capacitance of 15 pF

Modes	Experimental Results (MHz)	MRIEM (MHz)	FEM-EFAT (MHz)
m=4	182.1	189.53	186.56
m=3	187.2	198.07	193.04
m=2	200.8	229.37	215.00
m=1	245.0	314.53	261.16
m=0	370.1	-	382.64

Table 5.4: Measured and calculated resonant modes of 8-leg high-pass birdcage coil for the capacitance of 7.5 pF

Modes	Experimental Results (MHz)	MRIEM (MHz)	FEM-EFAT (MHz)
m=4	256.0	299.68	270.36
m=3	266.0	313.17	279.23
m=2	294.0	362.66	308.76
m=1	334.26	497.32	368.01
m=0	516.0	-	553.02

Table 5.5: Measured and calculated resonant modes of 8-leg high-pass birdcage coil for the capacitance of 3.3 pF

Using these results, we can calculate the percentage error of the results of the two software tools relative to the values obtained experimentally using the formula

$$Error\ rate\ (\%) = 100 \times \left| \frac{f_{meas} - f_{calc}}{f_{meas}} \right| \tag{5.1}$$

where f_{meas} is the measured frequency in the experiment and f_{calc} is the calculated frequency using one of the software tools, MRIEM or FEM-EFAT. Percentage errors of the results of these software tools are shown in Figure 5.2.

As can be seen in Figure 5.2, resonant modes calculated using the FEM-EFAT are more accurate compared with the experimental results. For the worst case scenario, in which the used capacitance value is 3.3 pF with a tolerance of $\pm 0.25pF$ and the wavelength is comparable with the coil dimensions, our software tool calculates the resonance frequencies with a maximum of % 10 error, whereas MRIEM calculates the first resonant modes with % 50 error. As previously mentioned, when the wavelength is comparable with the coil dimensions, calculation of the resonant modes using lumped circuit element model will give unreliable results. We can see this phenomena in the MRIEM results given in Figure 5.2 as the capacitance used in the experiment decreases (or the resonance frequencies

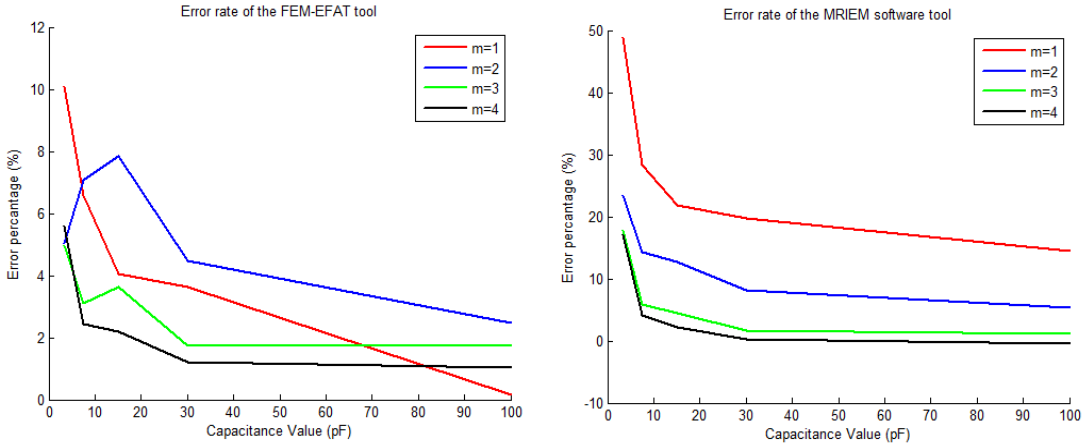

Figure 5.2: Percentage error rate of the two software tools: FEM-EFAT (left), MRIEM (right)

are increases), error in the calculated resonant modes significantly increases. Additionally, FEM-EFAT calculates the end ring resonant mode ($m = 0$), whereas MRIEM does not calculate the $m = 0$ mode.

5.1.2 Results of the Low-pass Birdcage Coil

Same as the high-pass birdcage coil results, the results of the resonant modes of the low-pass birdcage coil are given in a separate tables for five different capacitance values which are 47 pF ($\pm\%2$), 10 pF ($\pm\%2$), 3.3 pF ($\pm 0.25pF$), 1.8 pF ($\pm 0.25pF$), and 1 pF ($\pm 0.25pF$). Resonant modes results of the low-pass birdcage coil for these capacitance values are given in Table 5.6 to 5.10.

Modes	Experimental Results (MHz)	MRIEM (MHz)	FEM-EFAT (MHz)
m=1	60.75	67.46	59.1
m=2	85.88	90.64	87.22
m=3	93.38	102.2	101.1
m=4	102.8	-	105.4

Table 5.6: Measured and calculated resonant modes of 8-leg low-pass birdcage coil for the capacitance of 47 pF

Modes	Experimental Results (MHz)	MRIEM (MHz)	FEM-EFAT (MHz)
m=1	122.11	146.25	124.76
m=2	196.48	196.51	184.80
m=3	208.54	221.57	214.41
m=4	214.97	-	223.54

Table 5.7: Measured and calculated resonant modes of 8-leg low-pass birdcage coil for the capacitance of 10 pF

Modes	Experimental Results (MHz)	MRIEM (MHz)	FEM-EFAT (MHz)
m=1	211.3	254.59	205.37
m=2	306.3	342.08	306.62
m=3	330.0	385.71	356.47
m=4	345.0	-	371.75

Table 5.8: Measured and calculated resonant modes of 8-leg low-pass birdcage coil for the capacitance of 3.3 pF

Modes	Experimental Results (MHz)	MRIEM (MHz)	FEM-EFAT (MHz)
m=1	255.2	344.71	260.62
m=2	382.0	463.19	392.18
m=3	417.0	522.26	456.8
m=4	441.5	-	476.5

Table 5.9: Measured and calculated resonant modes of 8-leg low-pass birdcage coil for the capacitance of 1.8 pF

Modes	Experimental Results (MHz)	MRIEM (MHz)	FEM-EFAT (MHz)
m=1	335.7	462.48	316.85
m=2	473.1	621.42	481.6
m=3	512.3	700.68	562.24
m=4	525.9	-	586.63

Table 5.10: Measured and calculated resonant modes of 8-leg low-pass birdcage coil for the capacitance of 1 pF

According to these results, we can calculate the percentage error of the results of the software tools for each mode using the formula given in Equation 5.1 and this is illustrated in Figure 5.3.

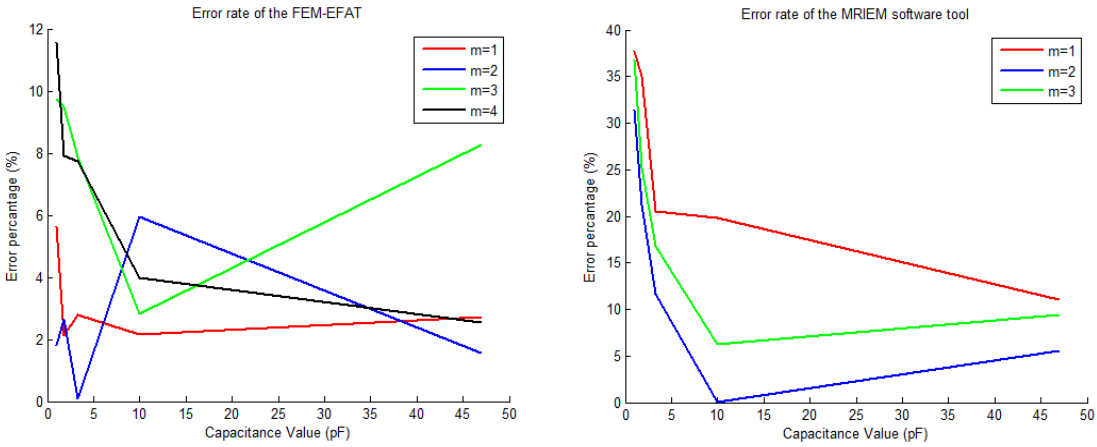

Figure 5.3: Percentage error rate of the two software tools: FEM-EFAT (left), BirdcageBuilder (right)

As can be seen in Figure 5.3, results of the FEM-EFAT is also more accurate than the results of MRIEM software tool in low-pass birdcage coils type. For the $m = 1$ mode, FEM-EFAT calculates the resonance frequencies with a maximum of % 8 error, whereas MRIEM calculates with % 37 error for the worst case. Additionally, FEM-EFAT calculates the singlet mode ($m = 4$) of the low-pass birdcage coil, whereas MRIEM does not calculate the singlet mode ($m = 4$) although its calculation is given in [9]. At last, error in the MRIEM results increases when the capacitance value decreases which is the same phenomena observed in the MRIEM results for the high-pass birdcage coil.

5.2 Used and Calculated Capacitance Values

In this section, we have estimated the necessary capacitance value for the same low-pass and high-pass birdcage coils for five different resonance frequencies. These are the measured resonance frequencies for the $m = 1$ mode corresponding to the capacitance values of 100 pF, 30 pF, 15 pF, 7.5 pF, and

3.3 pF for the high-pass birdcage coil, and corresponding to the capacitance values of 47 pF, 10 pF, 3.3 pF, 1.8 pF, and 1 pF for the low-pass birdcage coil used in the previous experiment. We have compared these capacitance values used in the experiments with the capacitance values calculated using two different software tools, which are our FEM based optimization tool (FEM-OPT) and BirdcageBuilder (a software tool that uses the lumped circuit element model presented in [5], and can be downloaded from the link, http://pennstatehershey.org/web/nmrlab/resources/software/birdcagebuilder). Results for the high-pass birdcage coil are given in Table 5.11.

Frequency	Experiment (pF)	BirdcageBuilder (pF)	FEM-OPT (pF)
75.25 MHz	100	99.27	100.34
131.4 MHz	30	32.56	32.3
182.5 MHz	15	16.88	16.03
245.0 MHz	7.5	9.36	8.65
334.26 MHz	3.3	5.03	4.2

Table 5.11: Used and calculated capacitance values of high-pass birdcage coil

Percentage error of the results of these two software tools can be calculated using the formula given as

$$Error\ rate\ (\%) = 100 \times \left| \frac{C_{exp} - C_{calc}}{C_{exp}} \right| \tag{5.2}$$

where C_{exp} and C_{calc} are the used and calculated capacitance respectively and it is illustrated in Figure 5.4.

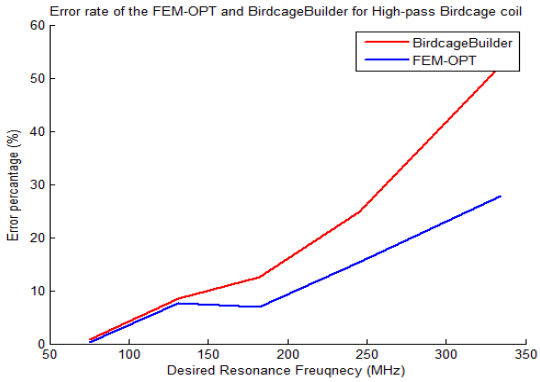

Figure 5.4: Percentage error of the software tools for the high-pass birdcage coil

As can be seen in Figure 5.4, error in the results of the both software tools increases when the desired frequency increases. However, increase in the error of the BirdcageBuilder results is significantly greater than the increase in the error of FEM-OPT results. Therefore, we can say that the results of the FEM-OPT is more accurate than the results of the BirdcageBuilder. For the worst case scenario, for example, FEM-OPT calculates the capacitance value with % 25 error, whereas BirdcageBuilder calculates with more than % 50 error. This is the expected result for the BirdcageBuilder since this method uses lumped circuit element model and inductance calculations will not be correct as the frequency increases.

Calculated capacitance values for the low-pass birdcage coil, on the other hand, are given in Table 5.12.

Frequency	Experiment (pF)	BirdcageBuilder (pF)	FEM-OPT (pF)
60.75 MHz	47	43.87	44.42
122.11 MHz	10	10.86	10.46
211.3 MHz	3.3	3.63	3.51
255.2 MHz	1.8	2.49	1.92
335.7 MHz	1	1.44	0.84

Table 5.12: Used and calculated capacitance values of low-pass birdcage coil

Using the formula given in Equation 5.2, percentage error of the results of the software tools for low-pass birdcage coil can be obtained as given in Figure 5.5.

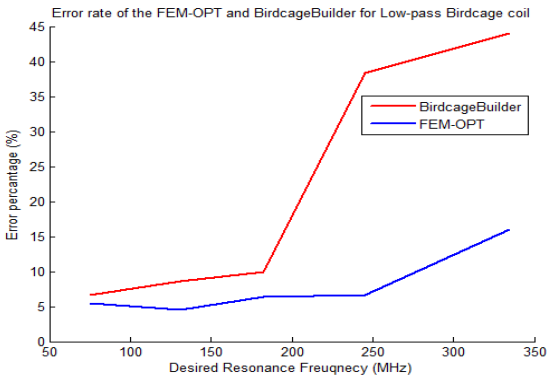

Figure 5.5: Percentage error of the software tools for the low-pass birdcage coil

Figure 5.5 shows that results of the FEM-OPT is also more accurate than

the results of the BirdcageBuilder for the low-pass birdcage coil. It is important to note that results for the capacitance values of 1 pF and 1.8 pF may not be taken into account, since the tolerance of these capacitances is ± 0.25 pF and this may affect the results significantly. Even if we do not take the results of these capacitances into consideration, results of FEM-OPT is still more accurate than the results of BirdcageBuilder.

Chapter 6

CONCLUSIONS

In this thesis, analysis of a birdcage coil using lumped circuit element model and using the developed 3D FEM models of low-pass and high-pass birdcage coils are explained. Three different FEM based simulation methods for designing and simulating the birdcage coils accurately in COMSOL Multiphysics are proposed.

In the design process, a new method for the capacitance calculation of a birdcage coil at the specified frequency is presented. In this method, we perform a FEM based optimization study using the magnitude of the port impedance of the birdcage coil model or the variance of the H^+ in the central region of the birdcage coil model as the objective function and the capacitance value as the control variable. As a consequence of this study, optimum capacitance value which maximizes (or minimizes) the objective function is calculated. Additionally, a software tool called FEM based OPtimization Tool (FEM-OPT) is developed in order to perform this method according to the user-specified parameters easily. Experimental results for the calculated capacitances show that the results of FEM-OPT are more accurate than the results of the other software tool (BirdcageBuilder) that uses lumped circuit element model. In low frequencies, where the coil dimensions is much smaller than the wavelength, the results of FEM-OPT and the results of BirdcageBuilder are almost the same. Therefore, users can use any of these software tools in order to calculate the capacitance value of a birdcage coil

for low frequencies. In high frequencies, however, where the wavelength is comparable with the coil dimensions, FEM-OPT gives more accurate results than the BirdcageBuilder. This is because the inductance calculations in lumped circuit element model are made under quasi-static assumptions and therefore error will increase as the desired resonance frequency increases. In FEM-OPT, on the other hand, we have made no assumptions while we are modeling the birdcage coils in the FEM simulation environment but we need to take into consideration of the size of the mesh elements. In order to obtain accurate results in FEM-OPT, maximum element size of the mesh elements must be at least one fifth of the wavelength.

In the simulation process, we have proposed two different electromagnetic analyses of birdcage coils. One of them is the frequency domain analysis and is used to solve for electromagnetic fields of a birdcage coil. By using this analysis, we can observe the electromagnetic fields inside the birdcage coil for any scenario such as loaded or shielded birdcage coil. Furthermore, this analysis can be used to estimate SAR at any object inside the coil or can be used to produce simulated B_1 data. The other electromagnetic analysis is the eigenfrequency analysis and is used to determine the resonant modes of the birdcage coil. One can also observe the electromagnetic field or other electromagnetic variable distributions inside the coil at these resonant modes in the eigenfrequency analysis. Furthermore, quality factor for the loaded or unloaded birdcage coils can be calculated using this analysis. Additionally, in order to perform both analysis according to the user-specified parameters easily, software tool called FEM based Frequency Domain Analysis (FEM-FDA) and FEM based EigenFrequency Analysis (FEM-EFAT) is developed. Experimental results for the calculated resonant modes show that the results of the FEM-EFAT are more accurate than the results of the other software tool (MRIEM) that uses lumped circuit element model. Since MRIEM uses the lumped circuit element model same as the BirdcageBuilder, error in the results of MRIEM significantly increases as the frequency increases.

Consequently, FEM based simulation methods and the corresponding software tools, which are proposed in this thesis, can be used to design and simulate the low-pass and high-pass birdcage coils accurately. These methods can be easily

adapted to design and simulate other RF coils such as transverse electromagnetic (TEM) coils and phased-array coils.

Bibliography

[1] C. Hayes, W. Edelstein, J. Schenck, O. Mueller, and M. Eash, "An efficient, highly homogeneous radiofrequency coil for whole-body NMR imaging at 1.5 T," *Journal of Magnetic Resonance*, vol. 63, pp. 622–628, 1985.

[2] C. Chen, D. Hoult, and V. Sank, "Quadrature detection coils–a further $\sqrt{2}$ improvement in sensitivity," *Journal of Magnetic Resonance*, vol. 54, pp. 324–327, 1983.

[3] M. C. Leifer, "Resonant modes of the birdcage coil," *Journal of Magnetic Resonance*, vol. 124, pp. 51–60, 1997.

[4] G. Giovannetti, L. Landini, M. Santarelli, and V. Positano, "A fast and accurate simulator for the design of birdcage coils in MRI," *Magnetic Resonance Materials in Physics, Biology and Medicine*, vol. 15, pp. 36–44, 2002.

[5] C.-L. Chin, C. M. Collins, S. Li, B. J. Dardzinski, and M. B. Smith, "Birdcagebuilder: Design of specified-geometry birdcage coils with desired current pattern and resonant frequency," *Concepts in Magnetic Resonance*, vol. 15, no. 2, pp. 156–163, 2002.

[6] J. Tropp, "The theory of the bird-cage resonator," *Journal of Magnetic Resonance*, vol. 82, no. 1, pp. 51–62, 1989.

[7] R. Pascone, B. Garcia, T. Fitzgerald, T. Vullo, R. Zipagan, and P. Cahill, "Generalized electrical analysis of low-pass and high-pass birdcage resonators," *Magnetic Resonance Imaging*, vol. 9, no. 3, pp. 395 – 408, 1991.

[8] A. Deutsch, G. Kopcsay, P. Restle, H. Smith, G. Katopis, W. Becker, P. Coteus, C. Surovic, B. Rubin, J. Dunne, R.P., T. Gallo, K. Jenkins, L. Terman, R. Dennard, G. Sai-Halasz, B. Krauter, and D. Knebel, "When are transmission-line effects important for on-chip interconnections?," *Microwave Theory and Techniques, IEEE Transactions on*, vol. 45, pp. 1836 –1846, oct 1997.

[9] J. Jin, *Electromagnetic Analysis and Design in Magnetic Resonance Imaging*. CRC Press, 1989.

[10] C. Guclu, G. Kashmar, O. Nalcioglu, and A. Hacinliyan, "An FEM approach for the characterization of the RF field homogeneity at high field," *Magnetic Resonance in Medicine*, vol. 37, no. 1, pp. 76–83, 1997.

[11] T. S. Ibrahim, C. Mitchell, P. Schmalbrock, R. Lee, and D. W. Chakeres, "Electromagnetic perspective on the operation of RF coils at 1.511.7 Tesla," *Magnetic Resonance in Medicine*, vol. 54, no. 3, pp. 683–690, 2005.

[12] W. Liu, C. Collins, and M. Smith, "Calculations of B_1 distribution, specific energy absorption rate, and intrinsic signal-to-noise ratio for a body-size birdcage coil loaded with different human subjects at 64 and 128 mhz," *Applied Magnetic Resonance*, vol. 29, pp. 5–18, 2005.

[13] C. A. T. V. den Berg, L. W. Bartels, B. van den Bergen, H. Kroeze, A. A. C. de Leeuw, J. B. V. de Kamer, and J. J. W. Lagendijk, "The use of MR B_1^+ imaging for validation of FDTD electromagnetic simulations of human anatomies," *Physics in Medicine and Biology*, vol. 51, no. 19, p. 4735, 2006.

[14] F. W. Grover, *Inductance Calculations*. Dover Publications, Inc., 2004.

[15] *RF Module User's Guide*. COMSOL AB, COMSOL 4.2, May 2011.

[16] Y. Duan, T. S. Ibrahim, B. S. Peterson, F. Liu, and A. Kangarlu, "Assessment of a PML Boundary Condition for Simulating an MRI Radio Frequency Coil," *International Journal of Antennas and Propagation*, vol. 2008, pp. 1–11, 2008.

[17] D. I. Hoult, "The principle of reciprocity in signal strength calculationsa mathematical guide," *Concepts in Magnetic Resonance*, vol. 12, no. 4, pp. 173–187, 2000.

[18] G. Anne, *Iterative Methods for Solving Linear Systems*. Society for Industrial and Applied Mathematics, 1997.

[19] P. Gill, W. Murray, and M. Saunders, "Snopt: An sqp algorithm for large-scale constrained optimization," *SIAM Review*, vol. 47, no. 1, pp. 99–131, 2005.

[20] K. Levenberg, "A method for the solution of certain non-linear problems in least squares," *Quarterly Journal of Applied Mathmatics*, vol. II, no. 2, pp. 164–168, 1944.

[21] D. W. Marquardt, "An algorithm for least-squares estimation of nonlinear parameters," *Journal of the Society for Industrial and Applied Mathematics*, vol. 11, no. 2, pp. 431–441, 1963.